AD_____

Award Number: DAMD17-97-1-7206

TITLE: P/CAF Function in Transcriptional Activation by Steroid Hormone Receptors and Mammary Cell Proliferation

PRINCIPAL INVESTIGATOR: Sharon Y. Roth, Ph.D.

CONTRACTING ORGANIZATION: The University of Texas,
MD Anderson Cancer Center
Houston, Texas 77030

REPORT DATE: July 2000

TYPE OF REPORT: Final

PREPARED FOR: U.S. Army Medical Research and Materiel Command
Fort Detrick, Maryland 21702-5012

REPORT DOCUMENTATION PAGE

Form Approved
OMB No. 074-0188

1. AGENCY USE ONLY (Leave blank)	2. REPORT DATE	3. REPORT TYPE AND DATES COVERED
	July 2000	Final (1 Jul 97 - 30 Jun 00)

4. TITLE AND SUBTITLE
P/CAF Function in Transcriptional Activation by Steroid Hormone Receptors and Mammary Cell Proliferation

5. FUNDING NUMBERS
DAMD17-97-1-7206

6. AUTHOR(S)
Sharon Y. Roth, Ph.D.

7. PERFORMING ORGANIZATION NAME(S) AND ADDRESS(ES)
The University of Texas, MD Anderson Cancer Center
Houston, Texas 77030

E-MAIL:
syr@mdacc.tmc.edu

8. PERFORMING ORGANIZATION REPORT NUMBER

9. SPONSORING / MONITORING AGENCY NAME(S) AND ADDRESS(ES)
U.S. Army Medical Research and Materiel Command
Fort Detrick, Maryland 21702-5012

10. SPONSORING / MONITORING AGENCY REPORT NUMBER

11. SUPPLEMENTARY NOTES

12a. DISTRIBUTION / AVAILABILITY STATEMENT
Approved for public release; distribution unlimited

12b. DISTRIBUTION CODE

13. ABSTRACT *(Maximum 200 Words)*

The purpose of this research is to investigate the role of histone acetyltransferases in the estrogen responses and the development and progression of breast tumors. Experiments were initially focused on one of these enzymes, PCAF. We have completed the major goals outlined in our original Statement of Work. Our studies have revealed that another acetylase, GCN5, is very highly related in both structure in and function to PCAF. However, loss of these two enzymes has dramatically different effects in mice. PCAF null mice are viable, fertile, and exhibit no defects in estrogen dependent processes. However loss of GCN5 leads to embryonic lethality due to loss of increased programmed cell death of mesodermal tissues. Moreover, GCN5 is genetically linked to BRCA1 and provides a candidate for a tumor suppressor gene associated with spontaneous breast and ovarian cancers. Combined mutations in PCAF and GCN5 have even more severe effects on mouse development. These results suggest that both GCN5 and PCAF are important to embryogenesis. Gcn5 is also important to the regulation of apoptosis and may play a role in tumor development.

14. SUBJECT TERMS	15. NUMBER OF PAGES
Breast Cancer	39
	16. PRICE CODE

17. SECURITY CLASSIFICATION OF REPORT	18. SECURITY CLASSIFICATION OF THIS PAGE	19. SECURITY CLASSIFICATION OF ABSTRACT	20. LIMITATION OF ABSTRACT
Unclassified	Unclassified	Unclassified	Unlimited

FOREWORD

Opinions, interpretations, conclusions and recommendations are those of the author and are not necessarily endorsed by the U.S. Army.

_N/A__ Where copyrighted material is quoted, permission has been obtained to use such material.

_N/A__ Where material from documents designated for limited distribution is quoted, permission has been obtained to use the material.

__N/A_ Citations of commercial organizations and trade names in this report do not constitute an official Department of Army endorsement or approval of the products or services of these organizations.

X In conducting research using animals, the investigator(s) adhered to the "Guide for the Care and Use of Laboratory Animals," prepared by the Committee on Care and use of Laboratory Animals of the Institute of Laboratory Resources, national Research Council (NIH Publication No. 86-23, Revised 1985).

N/A For the protection of human subjects, the investigator(s) adhered to policies of applicable Federal Law 45 CFR 46.

X In conducting research utilizing recombinant DNA technology, the investigator(s) adhered to current guidelines promulgated by the National Institutes of Health.

X In the conduct of research utilizing recombinant DNA, the investigator(s) adhered to the NIH Guidelines for Research Involving Recombinant DNA Molecules.

N/A In the conduct of research involving hazardous organisms, the investigator(s) adhered to the CDC-NIH Guide for Biosafety in Microbiological and Biomedical Laboratories.

7/10/00

PI - Signature Date

Table of Contents

Cover..... 1

SF 298..... 2

Foreword..... 3

Table of Contents..... 4

Introduction..... 5

Body..... 5

Key Research Accomplishments..... 6

Reportable Outcomes..... 7

Conclusions..... 7

References..... 8

Final report summary..... 9

Appendices..... 10

INTRODUCTION

Proliferation of mammary and uterine tissues is governed in large part by the steroid hormones (Beato et al., 1995), which trigger activation of genes that regulate the cell cycle (Kamei et al., 1996; Sicinski et al., 1995). Hormone binding stimulates receptor binding to response elements upstream of target genes. Gene activation by the steroid hormone receptors requires several cofactors, including the CREB binding protein (CBP) or the highly related p300 protein, as well as SRC-1, PCAF, and ACTR (Chen et al., 1997; Kamei et al., 1996; Onate et al., 1995; Spencer et al., 1997; Yang et al., 1996). Strikingly, all of these cofactors possess histone acetyltransferase activity. The histones fold DNA into chromatin and this folding is generally inhibitory to transcription. Post-translational acetylation of the histones modulates chromatin folding and is a key step in the regulation of gene expression (Turner, 1991; Wolffe and Pruss, 1996). Histone acetylation levels are governed by the opposing actions of two groups of enzymes, the histone acetyltransferases (HATs) and the histone deacetylases (HDACs). Experiments supported by this IDEA grant were focused on understanding the role of the PCAF histone acetyltransferase in steroid hormone responses in normal mammary development and in abnormal events that lead to cancer. Our original Specific Aims were to 1) complete the isolation and cloning of mouse PCAF cDNA and genomic sequences 2) to characterize murine PCAF as a histone acetyltransferase and 3) examine PCAF interactions with specific steroid receptors and CBP/p300 4) to examine whether acetylase activity is required for transcriptional activation by the hormone receptors 5) to create mice deficient for PCAF and mice that overexpress this factor to assess the role of PCAF in mouse development, differentiation, and tumorigenesis.

BODY

Specific Aim 1: to complete the isolation and cloning of mouse PCAF cDNA and genomic sequences. As reported previously, this specific aim was completed and the cloning of the mouse PCAF cDNA and genomic sequences was reported in a paper we published in *Molecular and Cellular Biology* (Xu et al, 1998; attached in appendix; see Figs. 1, 2, and 3). This paper also reports the cloning of a highly related gene encoding the GCN5 histone acetyltransferase and our finding that GCN5 is genetically linked to the BRCA1 locus.

Specific Aim 2: to characterize murine PCAF as a histone acetyltransferase. This specific aim was also completed, as reported previously. The results are depicted in Figs. 6 and 7 of Xu et al, 1998 (attached in appendix).

Specific Aim 3: to examine PCAF interactions with specific steroid receptors and CBP/p300. As reported last year, we and others have described the binding of PCAF to CBP/p300 (Xu et al, 1998 and (Yang et al., 1996)). Tissue culture experiments have been performed by others to examine the importance of PCAF to hormone responses (Chen et al., 1997), and they have found that PCAF augments estrogen responses. Our basic premise, then, that PCAF is important for these processes is supported by these cell culture results. However, our results below with the PCAF knock out mice indicate that PCAF is not required for these processes in whole animals. Therefore, we have completed all the relevant experiments in this aim and PCAF interactions with the hormone receptors will not be pursued further.

Specific Aim 4: to examine whether PCAF acetylase activity is required for transcriptional activation by the hormone receptors. As reported last year, these experiments were superceded by our findings with the PCAF knockout mice, which indicate PCAF is not needed for hormone responses in

mice. We proposed last year to modify this aim to make 'acetylase minus' forms of GCN5 for gene replacement studies in mice. We have now completed the cloning of these mutations and are now assembling them into our gene replacement vector.

Specific Aim 5: to create mice deficient for PCAF and mice that overexpress this factor to assess the role of PCAF in mouse development, differentiation, and tumorigenesis. As reported last year, the first half of this aim, to create PCAF deficient mice, is completed. Since PCAF and GCN5 are very highly related, we also created mice deficient for GCN5. Our creation and analysis of these mice is reported in a manuscript recently accepted for publication in *Nature Genetics* (Xu et al, 2000; manuscript attached in appendix). We found that loss of PCAF had no adverse effects on mouse development (see Fig. 1 in Xu et al, 2000) or in adult mice. Estrogen-regulated processes such as pregnancy and lactation were also unaffected. In contrast, loss of the highly related GCN5 protein causes embryonic lethality (see Fig. 2, Xu et al, 2000). We determined that this lethality is due to an increase in programmed cell death of particular mesodermal lineages. These exciting results suggest that GCN5 regulates apoptosis and thus, is likely be important in regulation of tumor formation or growth.

To relate the above accomplishments to our **Statement of Work**:

- **year 1:** All goals were completed except for the last one, to clone an MMTV-PCAF transgene. This goal became when we determined that our PCAF deficient mice exhibit no abnormal phenotype.
- **year 2:** All goals were completed, except for the last one, which again involves the MMTV-PCAF transgene.
- **year 3:** Goal 1 is still in progress; we are now cloning 'knock in vectors' for PCAF and GCN5 that will contain either wild type or 'acetylase minus' versions of these genes. Goal 2 is also completed. We monitored the PCAF knock out mice for spontaneous tumors for more than 2 years but saw no increased incidence or rate of tumor formation. Goal 3, to examine mammary tissue in the PCAF knock out mice, was completed and reported previously. We are now cloning of a breast-specific knock out vector for GCN5 (revised goal 4). When these mice are created, we will examine the expression and functions of the steroid receptors (goal5). These remaining experiments are now supported by a new grant from the USAMRC (see below).

KEY RESEARCH ACCOMPLISHMENTS

Reported in Xu et al, 1998:

- Isolation and cloning of the murine PCAF and GCN5 genes.
- Determination that both PCAF and GCN5 interact with CBP/p300
- Determination that GCN5 exists in a long and short form in mammalian cells
- Determination that GCN5 and PCAF have identical substrate specificities
- Determination that GCN5 and PCAF are expressed in complementary patterns in adult mice
- Determination that GCN5 is genetically linked to the BRCA1 locus

Reported in Xu et al, 2000

- Determination that PCAF is dispensable in mice
- Determination that GCN5 is essential for mouse development
- Determination that double mutations in GCN5 and PCAF cause more severe defects in mouse development than does loss of either gene alone, indicating that both HATs contribute to normal embryogenesis.
- Detemination that specific mesodermal lineages are missing in the GCN5 mutant mice

- Determination that loss of mesodermal lineages in the absence of GCN5 is due to a 25 fold increase in apoptosis in these tissues.

REPORTABLE OUTCOMES

Manuscripts:

1). Xu, W., Edmondson, D. G., and Roth, S.Y. (1998). Mammalian GCN5 and PCAF acetyltransferases have homologous amino terminal domains important for recognition of nucleosomal substrates. Molecular and Cellular Biology 18, 5659-5669

2) Xu, W., Edmondson, D.G., Evrard, Y.A., Wakamiya, M., Behringer, R.R., and Roth, S.Y. (2000). Loss of Gcn5 leads to increased apoptosis and mesodermal defects during mouse development. *Nature Genetics*, in press.

Abstracts:

Evrard, Y. Xu, W., Edmondson, D.G., Wakamiya, M., Behringer, R.R., and Roth, S.Y. Role of GCN5 in apoptosis, tumor suppression and breast development; presented at the DOD, USAMRMC Era of Hope Meeting, Atlanta, Georgia, June 8-12, 2000.

Evrard, Y. Xu, W., Edmondson, D.G., Wakamiya, M., Behringer, R.R., and Roth, S.Y. Analysis of mice null for two highly related histone acetyltransferases; presented at the Southwest Regional Society for Developmental Biology Meeting, Houston, Texas, March 10-13, 2000

Degrees obtained:

The Ph.D. thesis research of my former student, Wanting Xu, was supported largely by this grant, although she had a private fellowship that paid her stipend. Dr. Xu completed her Ph.D. in May, 1999. Another Ph.D. student, Anjanette Watson, was also supported partially by this grant. Anjie completed her Ph.D. in May, 2000.

Funding obtained:

Based in part on the results reported here, I was awarded another IDEA grant entitled "Role of GCN5 in estrogen response, tumor suppression, and breast development in mice' (BC990781), which began in June 2000. I have also received funding to study the importance of GCN5 in regulating apoptosis during normal fetal development in mice from the March of Dimes Foundation (FY00-176).

CONCLUSIONS

We discovered that the PCAF gene is very highly related in structure and in function to the GCN5 gene. However, loss of these two genes has very different consequences in the mouse. PCAF is apparently dispensable. This result is especially surprising because a number of studies in tissue culture cells indicate that PCAF is important to hormone responses, including estrogen responses, and to muscle cell

differentiation. The absence of abnormalities in hormone dependent processes in PCAF deficient mice indicates either that PCAF is not important for these processes or that redundant activities, like GCN5, 'fill in' when PCAF is missing. In contrast, loss of GCN5 results in embryonic death due to an increase in apoptosis. This finding further supports the idea that GCN5 and PCAF may be important for regulation of tumorigenesis, since programmed cell death is often altered in tumor cells. We have also found that GCN5 is genetically linked to BRCA1 in mouse. Others have found this same linkage in humans. This region of the human genome often exhibits loss of heterozygosity in spontaneous breast and ovarian cancers, which do not exhibit mutations in BRCA1 or BRCA2. We are now investigating how GCN5 regulates apoptosis, how this regulation might be tied to tumorigenesis, and how, or if, GCN5 is important to mammary development. These experiments are important for discerning how histone acetyltransferases contribute to hormone responses and apoptosis, and thus may yield invaluable information for the prevention or treatment of hormone responsive breast cancers.

REFERENCES

Beato, M., Herlich, P., and Schutz, G. (1995). Steroid hormone receptors: many actors in search of a plot., Cell *83*, 851-857.

Chen, H., Lin, R. J., Schlitz, R. L., Chakravarti, D., Nash, A., Nagy, L., Privalsky, M. L., Nakatani, Y., and Evans, R. M. (1997). Nuclear receptor coactivator ACTR is a novel histone acetyltransferase and forms a multimeric activation complex with PCAF and CBP/p300., Cell *90*, 569-580.

Kamei, Y., Xu, L., Heinzel, T., Torchia, J., Kurokawa, R., Gloss, B., Lin, S., Heyman, R. A., Rose, D. W., Glass, C. K., and Rosenfeld, M. G. (1996). A CBP integrator complex mediates transcriptional activation and AP-1 inhibition by nuclear receptors., Cell *85*, 403-414.

Onate, S. A., Tsai, S. Y., Tsai, M. J., and O'Malley, B. W. (1995). Sequence and characterization of a coactivator for the steroid hormone receptor superfamily., Science *270*, 1354-1357.

Sicinski, P., Donaher, J. L., Parker, S. B., Li, T., Fazeli, A., Gardner, H., Haslam, S. Z., Bronson, R. T., Elledge, S. J., and Weinberg, R. A. (1995). Cyclin D1 provides a link between development and oncogenesis in the retina and the breast., Cell *82*, 621-630.

Spencer, T. E., Jenster, G., Burcin, M. M., Allis, C. D., Zhou, J., Mizzen, C. A., McKenna, N. J., Onate, S. A., Tsai, M. J., and O'Malley, B. W. (1997). Steroid receptor coactivator-1 is a histone acetyltransferase, Nature *389*, 194-198.

Turner, B. M. (1991). Histone acetylation and control of gene expression, Journal of Cell Science *99*, 13-20.

Wolffe, A. P., and Pruss, D. (1996). Targeting chromatin disruption: Transcription regulators that acetylate histones, Cell *84*, 817-9.

Yang, X.-J., Ogryzko, V. V., Nishikawa, J.-I., Howard, B. H., and Nakatani, Y. (1996). A p300/CBP associated factor that competes with the adenoviral oncoprotein E1A, Nature *382*, 319-324.

FINAL REPORT

Bibliography:

1). Xu, W., Edmondson, D. G., and Roth, S.Y. (1998). Mammalian GCN5 and PCAF acetyltransferases have homologous amino terminal domains important for recognition of nucleosomal substrates. Molecular and Cellular Biology 18, 5659-5669

2) Xu, W., Edmondson, D.G., Evrard, Y.A., Wakamiya, M., Behringer, R.R., and Roth, S.Y. (2000). Loss of Gcn5 leads to increased apotosis and mesodermal defects during mouse development. *Nature Genetics*, in press.

Meeting Abstracts:

Evrard, Y. Xu, W., Edmondson, D.G., Wakamiya, M., Behringer, R.R., and Roth, S.Y. Role of GCN5 in apoptosis, tumor suppression and breast development; presented at the DOD, USAMRMC Era of Hope Meeting, Atlanta, Georgia, June 8-12, 2000.

Evrard, Y. Xu, W., Edmondson, D.G., Wakamiya, M., Behringer, R.R., and Roth, S.Y. Analysis of mice null for two highly related histone acetyltransferases; presented at the Southwest Regional Society for Developmental Biology Meeting, Houston, Texas, March 10-13, 2000

Personnel who received pay from this grant:

Sharon Roth
Anjanette Watson
Diane Edmondson
Geraldine Srajer
Yukio Mukai
James Bone
Suhyun An
Huy Phan
Yvonne Evrard

APPENDIX

Publications

1). Xu, W., Edmondson, D. G., and Roth, S.Y. (1998). Mammalian GCN5 and PCAF acetyltransferases have homologous amino terminal domains important for recognition of nucleosomal substrates. Molecular and Cellular Biology 18, 5659-5669

2) Xu, W., Edmondson, D.G., Evrard, Y.A., Wakamiya, M., Behringer, R.R., and Roth, S.Y. (2000). Loss of Gcn5 leads to increased apoptosis and mesodermal defects during mouse development. *Nature Genetics*, in press.

MOLECULAR AND CELLULAR BIOLOGY, Oct. 1998, p. 5659–5669 Vol. 18, No. 10
0270-7306/98/$04.00+0

Mammalian GCN5 and P/CAF Acetyltransferases Have Homologous Amino-Terminal Domains Important for Recognition of Nucleosomal Substrates

WANTING XU, DIANE G. EDMONDSON, AND SHARON Y. ROTH*

Department of Biochemistry and Molecular Biology, University of Texas M. D. Anderson Cancer Center, Houston, Texas 77030

Received 4 November 1997/Returned for modification 22 December 1997/Accepted 5 June 1998

The yeast transcriptional adapter Gcn5p serves as a histone acetyltransferase, directly linking chromatin modification to transcriptional regulation. Two human homologs of Gcn5p have been reported previously, hsGCN5 and hsP/CAF (p300/CREB binding protein [CBP]-associated factor). While hsGCN5 was predicted to be close to the size of the yeast acetyltransferase, hsP/CAF contained an additional 356 amino-terminal residues of unknown function. Surprisingly, we have found that in mouse, both the *GCN5* and the *P/CAF* genes encode proteins containing this extended amino-terminal domain. Moreover, while a shorter version of GCN5 might be generated upon alternative or incomplete splicing of a longer transcript, mRNAs encoding the longer protein are much more prevalent in both mouse and human cells, and larger proteins are detected by GCN5-specific antisera in both mouse and human cell extracts. Mouse *GCN5* (*mmGCN5*) and *mmP/CAF* genes are ubiquitously expressed, but maximum expression levels are found in different, complementary sets of tissues. Both mmP/CAF and mmGCN5 interact with CBP/p300. Interestingly, *mmGCN5* maps to chromosome 11 and cosegregates with *BRCA1*, and *mmP/CAF* maps to a central region of chromosome 17. As expected, recombinant mmGCN5 and mmP/CAF both exhibit histone acetyltransferase activity in vitro with similar substrate specificities. However, in contrast to yeast Gcn5p and the previously reported shorter form of hsGCN5, mmGCN5 readily acetylates nucleosomal substrates as well as free core histones. Thus, the unique amino-terminal domains of mammalian P/CAF and GCN5 may provide additional functions important to recognition of chromatin substrates and the regulation of gene expression.

Transcription is a complex process requiring the coordinate action of multiple basal and transactivating proteins. In eukaryotic cells, this process is complicated further by the packaging of DNA into chromatin. Nucleosomes provide the fundamental repeat unit of chromatin, consisting of two molecules of each of the four core histones (H2A, H2B, H3, and H4) and ~146 bp of DNA wound in almost two turns around the exterior of the histone octamer (37). Individual nucleosomes as well as more highly folded structures are generally inhibitory to the initiation of transcription. Alterations in nucleosomal structure and in chromatin packing often accompany transcriptional activation (12).

Posttranslational acetylation of the histones has long been correlated with transcriptional activation (36, 39, 40). Acetylation neutralizes the charge associated with epsilon amino groups of lysine residues, thereby loosening contacts between the histones and the negatively charged DNA. Histone acetylation also influences compaction of nucleosomal arrays, yielding less condensed chromatin structures (16). Both of these effects can increase transactivator binding to nucleosomal DNA, facilitating transcriptional activation.

A molecular basis for the linkage between histone acetylation and gene activation was provided by the discovery that the yeast transcriptional adapter Gcn5p serves as the catalytic subunit of a histone acetyltransferase type A activity (5). Gcn5p is associated with two multisubunit complexes in yeast, which include Ada proteins (Ada2p, Ada3p, and Ada5p) and/or certain Spt proteins (6, 14, 18, 24, 25, 31). These complexes are required for transcriptional activation by particular transactivators, including heterologous VP16 derivatives and endogenous Gcn4p (3, 13, 24, 34). Components of the Gcn5p-Adap complex contact both transactivator proteins and basal transcription proteins, thus providing an adapter or coactivator function, in addition to histone acetyltransferase activity (2, 34). Association with both Ada2p and acetyltransferase activity is required for Gcn5p function in vivo (8, 38).

Human homologs of *GCN5* have been cloned based on sequence and functional similarities of their predicted products to the yeast protein. A cDNA predicted to encode a protein of similar size and with overall homology to yeast Gcn5p has been described (7, 41). A human *ADA2* gene has also been cloned, indicating a conservation of adapter and histone acetyltransferase functions across species (7). In addition, a cDNA encoding a second, larger Gcn5-related protein that possesses unique sequences in its amino-terminal half has been identified. This protein, P/CAF (p300/CREB binding protein [CBP]-associated factor), associates with two highly related proteins, p300 and CBP, that have a region of homology with ADA2 (41). Interestingly, p300 and CBP are also histone acetyltransferases (1, 29). Interactions between P/CAF and p300 or CBP are disrupted by the viral E1A oncogene product, and this disruption is required for cellular transformation by E1A (41). Proper association of these histone acetyltransferase activities, then, is extremely important for normal cell growth (32).

In order to further study the functions of histone acetyltransferases in the growth and development of mammalian cells, we endeavored to isolate sequences encoding mouse GCN5 (mmGCN5) and mmP/CAF. To our surprise, although our

* Corresponding author. Mailing address: Department of Biochemistry and Molecular Biology, University of Texas M. D. Anderson Cancer Center, Houston, TX 77030. Phone: (713) 794-4908. Fax: (713) 790-0329. E-mail: syr@mdacc.tmc.edu.

mmGCN5 exhibited 98% identity with the reported human *GCN5* (hsGCN5) sequence, the mouse cDNA encoded an extended amino-terminal domain with high similarity to a corresponding domain in P/CAF. Upon further examination, we found that the reported *hsGCN5* cDNA (41) may result from an incompletely spliced transcript, and that a more prevalent transcript exists that potentially encodes a longer hsGCN5 protein similar to that encoded by the mouse cDNA that we isolated. Moreover, in contrast to previous reports that yeast and human GCN5 proteins acetylate only free core histones, the full-length recombinant mmGCN5 protein containing this extended amino-terminal region acetylates both free and nucleosomal histones H3 and H4. These results suggest that this additional domain in the mammalian GCN5 acetyltransferase facilitates chromatin recognition. Interestingly, P/CAF and GCN5 are expressed in inverse ratios in many mouse tissues, indicating that these proteins may serve tissue-specific functions.

MATERIALS AND METHODS

cDNA library screening. Nested PCR with degenerate oligomers and a mouse embryonic cDNA library (13.5 days postcoitum [dpc]) as the template was performed to generate a fragment of the *mmGCN5* cDNA. Oligomers were chosen from regions of sequence conserved between yeast and *Tetrahymena*,[1] which correspond to amino acids 131 to 244 of the yeast protein sequence. A single band of 123 bp was generated and cloned into pBluescript (Stratagene). Sequencing revealed 80% nucleotide identity and 94% identity at the amino acid level to the reported hsGCN5. This PCR product and human EST clones (IMAGE clone no. 243927) with similarity to GCN5 were used together to screen a cDNA library under conditions of low stringency as previously described (11). Clones were plaque purified and rescued as per the manufacturer's protocol. Sequencing revealed two types of clones, some with similarity to *hsGCN5* and some with similarity to *hsP/CAF*. All of the *P/CAF* clones contained only a short piece of *P/CAF*, and rescreening of the library failed to isolate any longer clones. Therefore, an oligomer corresponding to the 5′-most sequence of *mmP/CAF* was used to screen a 10.5-dpc embryonic mouse plasmid library with GeneTrapper technology (Gibco BRL). Additional clones, corresponding to full-length *P/CAF* sequences, were isolated according to the manufacturer's protocol.

Genomic library screening. A mouse genomic library, Lambda FIXII (Stratagene), was screened by using a mixture of a 5′ fragment of the *mmGCN5* cDNA and a 5′ fragment of the *mmP/CAF* cDNA. Positive plaques were picked and subjected to secondary screening. Phage DNA was prepared from positive plaques by standard procedures. Genomic inserts were released from phage DNA by *Not*I digestion and subsequently subcloned into Bluescript KS(+) (Stratagene).

Sequencing analysis. DNA sequencing was performed by using the Thermo-Sequenase radiolabeled terminator cycle sequencing kit (Amersham Life Science). Sequencing amplification conditions were 94°C for 30 s, 55°C for 30 s, and 72°C for 1 min for 40 cycles. Alternatively, automated sequencing was carried out by the Sequencing Core Facility at the M. D. Anderson Cancer Center.

Sequence alignment. Published sequences were obtained by searching the GenBank, PIR-Protein, and SWISS-PROT databases. Sequence alignment was carried out with the Genetics Computer Group (GCG) (Wisconsin Package version 9.1; GCG, Madison, Wis.) Pileup program. Percent identity between two proteins was calculated by using the GCG Bestfit program.

Linkage analysis mapping. Restriction fragment length polymorphisms for *mmGCN5* or *mmP/CAF* in C57BL/6J and SPRET/Ei subspecies were determined by using genomic DNA purchased from the Jackson Laboratory. The Jackson Laboratory interspecific backcross panel (C57BL/6JEi × SPRET/Ei)F_1 × SPRET/Ei, known as Jackson BSS (33), was then used to map the chromosomal locations of the *mmGCN5* and *mmP/CAF* genes. Predigested panels (*Bgl*II digestion for *P/CAF* or *Xba*I digestion for *GCN5*) were analyzed by Southern blotting with a *GCN5* or *P/CAF* intronic probe. Typing results were processed via the Jackson Laboratory database analysis (see http://www.jax.org/resources/documents/cmdata for raw data).

RT-PCR. Isolation of total RNA from various mouse tissues was performed as described previously (10). RNA was digested with RNase A-free DNase I (Ambion) for 30 min at 37°C. Reverse transcriptase PCR (RT-PCR) was performed with an RT-PCR kit (Perkin-Elmer) according to manufacturer's protocols. Reverse transcription was carried out at 42°C for 15 min, followed by heating at 95°C for 5 min. PCRs were carried out at 95°C for 60 s and 60°C for 60 s for 35 cycles as suggested by the manufacturer. Primer A (see Fig. 3B for sequence location) for RT-PCR is CTGGTGCCTGAGAAGAGGAC; primer B (see Fig. 3B) is CTCCGAAGGTGGCATGGTGAAG.

RNA analysis. Total RNA from adult mouse tissues or whole embryos (13.5 dpc) was extracted as described previously (10). RNAs were electrophoresed on a 1.1% agarose gel containing formaldehyde, along with RNA molecular size markers (Gibco BRL). RNA was transferred to a GeneScreen Plus membrane (NEN Life Science) in 10× SSC (1× SSC is 0.15 M NaCl plus 0.015 M sodium citrate). Hybridization was carried out with *mmGCN5*- and *mmP/CAF*-specific probes.

GCN5 protein analysis. Mouse embryos (12.5 dpc) were homogenized in radioimmunoprecipitation assay buffer (1× phosphate-buffered saline, 1% Nonidet P-40, 0.5% sodium deoxycholate, 0.1% sodium dodecyl sulfate [SDS], 100 μg of phenylmethylsulfonyl fluoride per ml, 1 μg of aprotinin per ml) and then centrifuged at 15,000 × *g* for 20 min at 4°C. Supernatant was collected for Western blotting, and GCN5 was immunoprecipitated with the polyclonal hsGCN5 antibody (generously provided by Shelley Berger, Wistar Institute) by the protocol of Santa Cruz Biotech, Inc. HeLa cell nuclear extract was kindly provided by Warren Liao and Yongsheng Ren (M.D. Anderson Cancer Center).

Cloning and expression of full-length *mmGCN5* and *mmP/CAF*. Comparison of the *mmGCN5* genomic and cDNA clones revealed that the isolated cDNA lacks the sequences encoding the first 74 amino acids. These sequences (which lack introns) were excised from the *GCN5* genomic clone by *Nco*I and *Bss*HII digestion and inserted into the appropriate position of the cDNA clone to generate a full-length *mmGCN5* cDNA, as verified by DNA sequencing. Full-length *mmGCN5* was subcloned into the *Nco*I and *Hin*dIII sites of the pRSETB vectors (Invitrogen), such that an N-terminal His_6 tag was fused in frame with the coding region. Similarly, full-length *mmP/CAF* was subcloned into the *Bam*HI and *Kpn*I sites of the pRSETB vector. His_6-tagged proteins were induced in BL21-DE3 bacterial cells by addition of 1 mM IPTG (isopropyl-β-D-thiogalactopyranoside). Recombinant protein was purified by using nickel-nitrilotriacetic acid resin (Qiagen) according to the manufacturer's protocol. Purified recombinant proteins were verified by Western blot analysis with an antibody specific to the His_6 tag (Clontech).

Acetyltransferase assays. Acetyltransferase assays were performed as previously described (4, 5). HeLa cell mononucleosomes or core histones were the kind gift of Jerry Workman, and the cysteine-linked peptides (corresponding to amino acids 1 to 20 of H3 or to this same region with substitution of acetyl-lysine at positions 9 and 14) were the gift of C. David Allis. Calf thymus histones were purchased from Worthington Biochemical Corporation (Freehold, N.J.). Acetylation assays were performed in 10- to 30-μl volumes with either 10 μg of histones or the indicated amount of synthetic peptide. Following incubation at 30°C for 30 min, an aliquot of each reaction mixture was processed for liquid scintillation counting (P81 filter assay) as described by Brownell et al. (5), and when appropriate, another aliquot was electrophoresed on an SDS–22% polyacrylamide gel and histones were visualized by Coomassie blue staining and autoradiography.

GST fusion protein interaction assays. Glutathione *S*-transferase (GST)–CBP/p300 interaction assays were performed as described by Yang et al. (41) except that crude bacterial lysates containing His-tagged recombinant P/CAF, GCN5, or HIRA were used and the interactions were detected by Western blotting with the His tag antibody.

RESULTS

Cloning of *mmGCN5*. In order to study the function of acetyltransferases in a mammalian system, we endeavored to clone mouse *GCN5* homologs. First we generated a fragment of the *mmGCN5* cDNA using a nested PCR strategy employing degenerate primers homologous to conserved regions of the yeast *GCN5* and the *Tetrahymena* p55 genes. To further enhance the probability of identifying *GCN5*-related sequences, this fragment was used together with a human *GCN5* EST to screen a 13.5-dpc mouse embryonic cDNA library under conditions of low stringency (11). Multiple positive clones were identified, and upon sequencing, these were found to contain open reading frames predicted to encode proteins with significant homology to either hsGCN5 or hsP/CAF (Fig. 1).

One cDNA clone contained an open reading frame encoding 756 amino acids, and the C-terminal portion of this predicted amino acid sequence exhibited 98% identity with the reported hsGCN5 sequence, but only 71% homology to the hsP/CAF sequence, over the length of the predicted proteins (Fig. 2A). We tentatively concluded that this cDNA clone likely contains the *mmGCN5* gene, as confirmed below.

We next used a fragment from the 5′ end of this clone to screen a library of mouse genomic sequences. Three different clones were isolated, and restriction analysis and sequencing indicated that all three clones harbored the entire *mmGCN5*

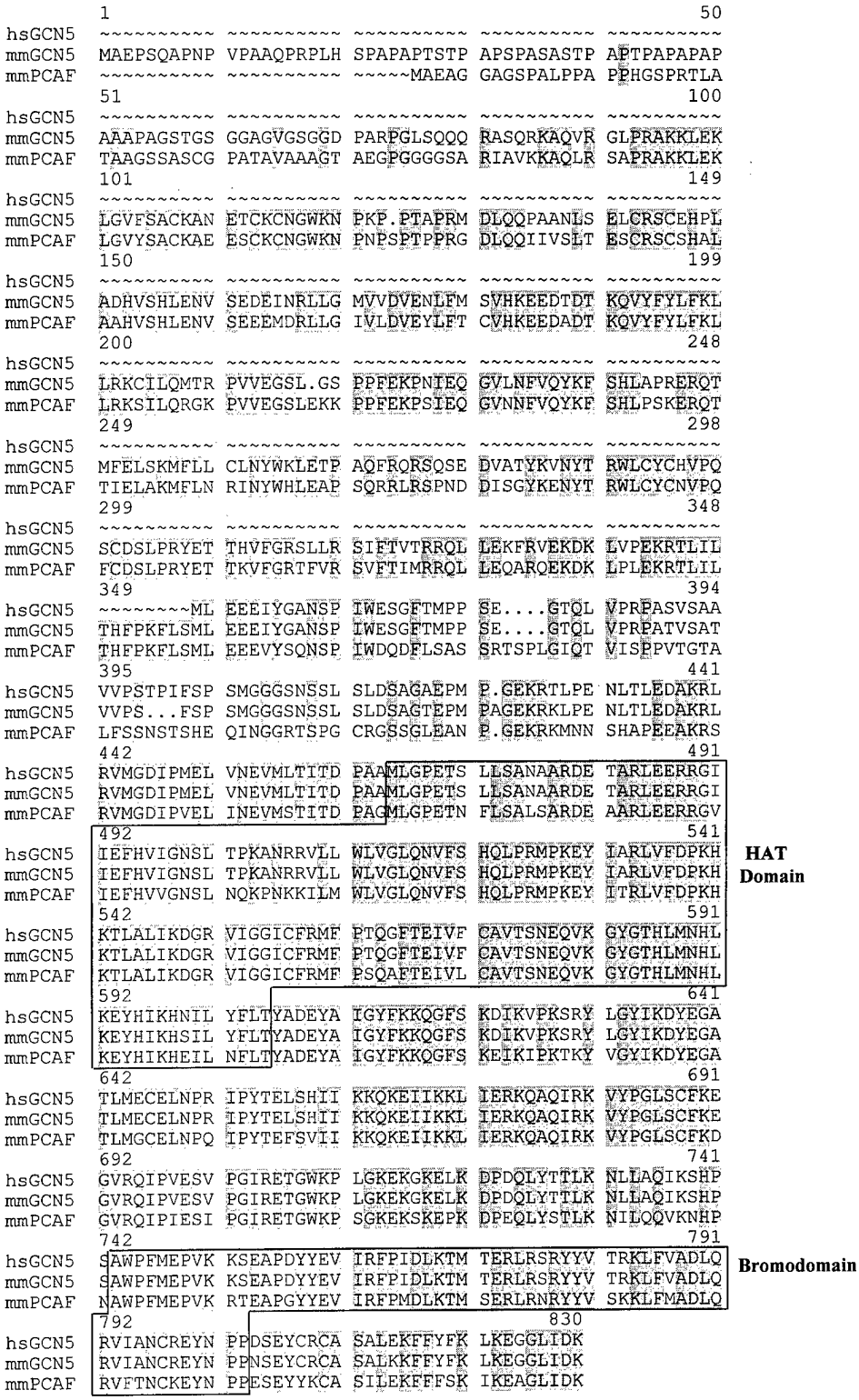

FIG. 1. Alignment of the mmGCN5, mmP/CAF, and reported hsGCN5 amino acid sequences. Identical amino acids are shaded. Amino acid deletions are indicated with a dotted line. The locations of the histone acetyltransferase (HAT)/acetyl coenzyme A binding regions (20, 38) and the bromodomain motif (17) are indicated. The full bromodomain likely encompasses amino acids 363 to 472 of hsGCN5 (19).

(A)

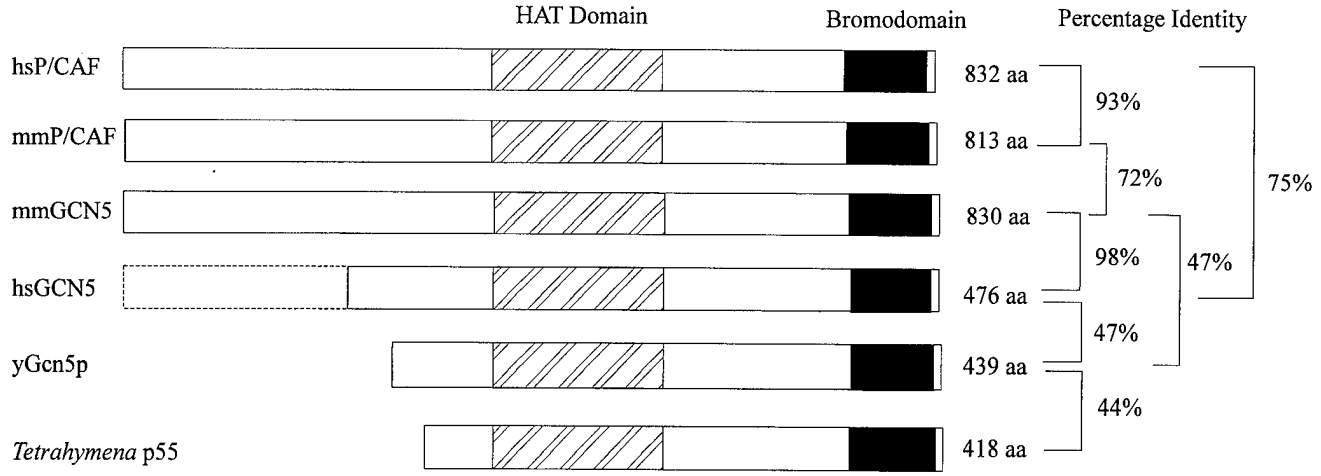

(B)

	−3 +4
Kozak consensus:	A/G CCAUGG
mouse GCN5 start site:	GCCAUGG
reported human GCN5 start site:	TCCAUGC

FIG. 2. Comparison of GCN5 and P/CAF sequences across species. (A) Schematic comparisons of mmGCN5 and mmP/CAF sequences with GCN5 and P/CAF proteins from other species. Published sequences were obtained by searching the PIR-Protein and SWISS-PROT databases. Positions of the putative catalytic domains and the bromodomains are indicated above the diagram. Percent identities between proteins are indicated on the right. yGcn5p, yeast Gcn5p; HAT, histone acetyltransferase; aa, amino acids. The dotted box indicates the existence of a predicted extended amino-terminal region in the hsGCN5 protein. (B) Comparison of the Kozak consensus sequence for translation start sites, the predicted mmGCN5 translation start sites, and the previously reported hsGCN5 translation start site (41). The underlined AUG is the codon for the initiator methionine. The A of the AUG is designated +1. In the consensus sequence, the nucleotides at positions −3 and +4 have the greatest impact on translation efficiency; 97% of vertebrate mRNAs have a purine (A or G, preferably A) in position −3, and 46% have a G in position +4 (21, 22).

gene. Comparison of the genomic and cDNA clones of *mmGCN5* revealed that the cDNA clone isolated as described above actually lacked the first 74 amino-terminal codons and that the *mmGCN5* gene is divided into 19 exons and contains relatively small (85-bp to 1-kb) introns (Fig. 3A). We inserted sequences from the genomic clone containing the missing amino-terminal codons into the cDNA clone to generate a full-length (encoding 830 amino acids) recombinant *mmGCN5* cDNA.

The two previously reported hsGCN5 sequences differ in the position of the initiating methionine, such that one reported sequence contains 49 additional amino-terminal amino acids relative to the other (7, 41). The *mmGCN5* open reading frame also encodes these additional amino acids, but the open reading frame is further extended for some distance upstream of these sequences, potentially encoding 356 additional amino acids. The context of the predicted translation initiation site in this extended region of *mmGCN5* matches well the Kozak consensus sequence (Fig. 2B) (21, 22). Moreover, the amino acids in this amino-terminal extension exhibit more than 66% identity to sequences in the corresponding regions of both mouse (see below) and human P/CAF, and the length of this extended region is similar to that of the P/CAF proteins. These data indicate that *mmGCN5* encodes a protein that is very homologous to yeast Gcn5p and is almost identical to the previously reported hsGCN5 but that contains an extended N-terminal domain homologous to P/CAF in both size and sequence.

Incomplete splicing might yield a shorter GCN5 protein in mouse and human cells. We were interested in determining the basis of the incongruity in size between *mmGCN5* and the reported human cDNA. Inspection of the *mmGCN5* genomic sequence revealed the presence of an intron (intron 6 in Fig. 3A) 10 bp upstream of the previously reported upstream-most hsGCN5 translation initiation site (41). Sequences highly similar (91% identical) to these intronic sequences are also present in the predicted 5′ untranslated region of the reported *hsGCN5* cDNA but are absent in the mouse cDNA we isolated as described above. These comparisons suggest either that the mouse and human *GCN5* genes are subject to differential splicing events, in which this intron is either removed (mouse) or retained (human), or that the previously identified human

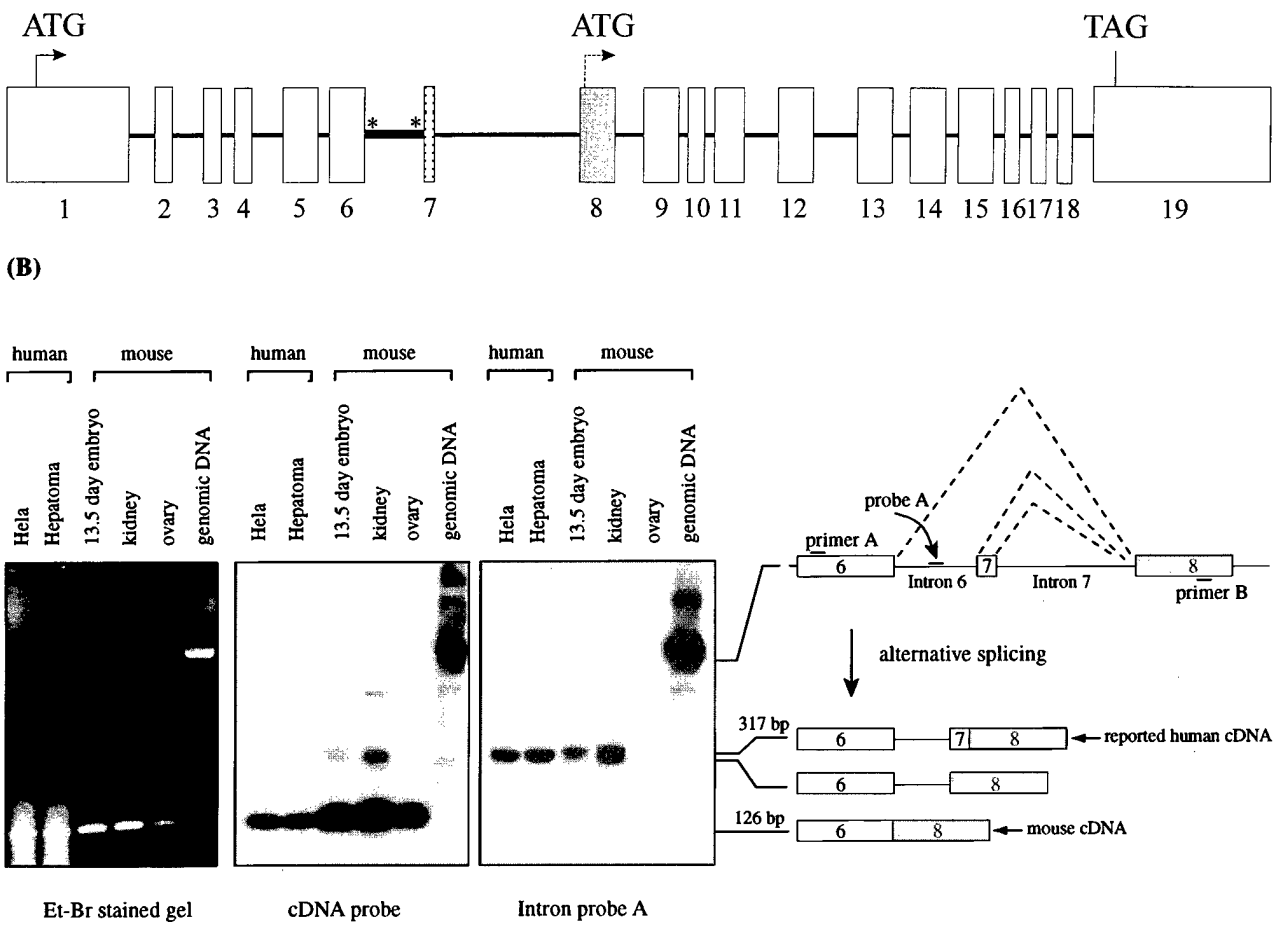

FIG. 3. (A) Genomic structure of *mmGCN5*. Exons in the *mmGCN5* gene are shown in boxes, while introns are represented by the intervening lines. The thick line indicates the intron that is retained in some alternatively spliced variants and which is homologous with sequences found in the previously reported 5′ untranslated region of the *hsGCN5* cDNA. The asterisks indicate in-frame stop codons that would prevent translation of the full-length protein. Exon 7 is the exon that is skipped in the mouse cDNA. Exon 8 is the first coding exon in the reported *hsGCN5* cDNA. The positions of the translation start codon (ATG) and the termination codon (TAG) are indicated. (B) Coexistence of multiple forms of mammalian *GCN5* transcripts. Left panel, DNase I-treated RNAs from mouse kidney, ovary, and embryo and human HeLa and hepatoma cell lines were RT-PCR amplified by using primers A and B shown in the diagram on the right. RT-PCR products were resolved on an ethidium bromide (Et-Br)-stained agarose gel. Mouse genomic DNA was also amplified under the same conditions. A prevalent product corresponding to the size of the mouse cDNA (without introns 6 and 7) was amplified from all of the RNA samples, while other, larger products corresponding to the size of the reported human cDNA (containing intron 6 but not intron 7) were barely detected. Middle panel, the RT-PCR products were transferred to nylon membrane and hybridized with *mmGCN5* cDNA sequences. Right panel, the same blot from the middle panel was stripped and rehybridized with a probe (probe A) specific to the conserved intron 6. (C) The RT-PCR products described above were gel purified and then amplified by PCR with a nested pair of primers. The PCR products were then subjected to DNA sequencing. The nucleotide sequence of the 317-bp fragment is shown. The smaller (292-bp) fragment has the same sequence as the larger fragment except that it lacks exon 7 sequences. Exons are boxed, and introns are numbered underneath. In-frame stop codons are in boldface and marked by asterisks. The *mmGCN5* reading frame separated by intron 6 and exon 7 is shown. The initiator methionine codon for the reported hsGCN5 (41) protein is in boldface and underlined.

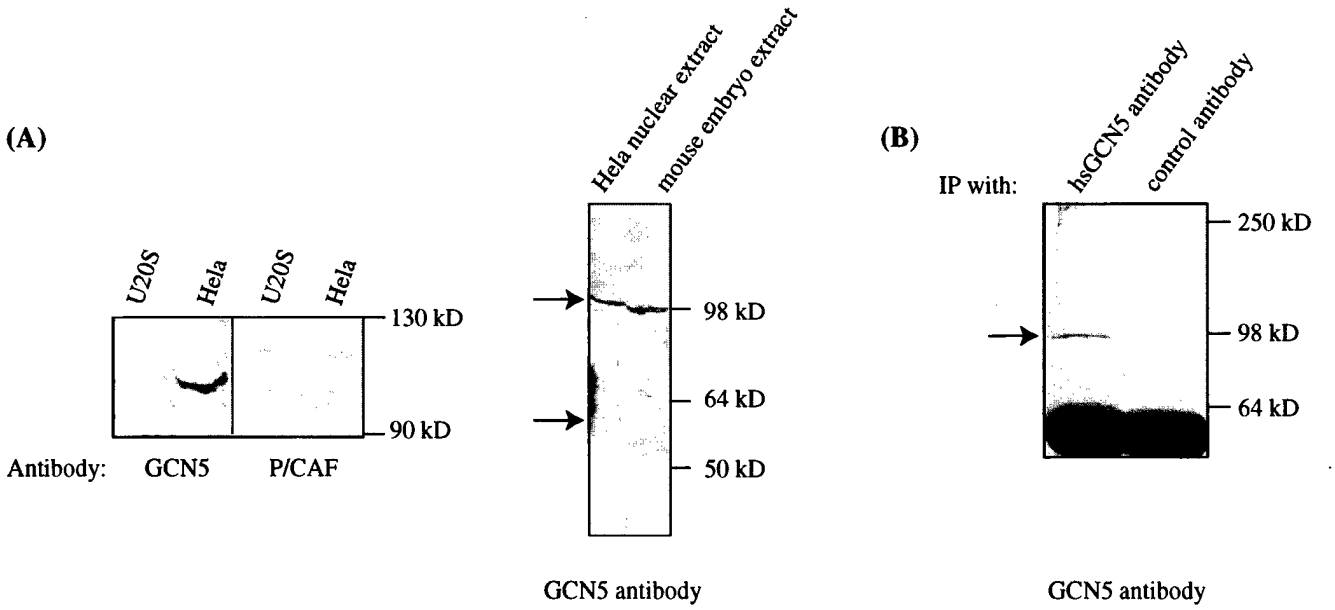

FIG. 4. Detection of both long and short GCN5 proteins. (A) Left panel, protein extracts were prepared from U2OS cells or HeLa cell nuclei and probed with polyclonal antibodies to hsP/CAF or hsGCN5, as indicated. Right panel, protein extracts were prepared from 12.5-dpc mouse embryos or HeLa cells and probed with the hsGCN5 antibody. (B) GCN5 proteins were immunoprecipitated (IP) from 12.5-dpc mouse embryos and then probed with hsGCN5 antibody. An unrelated HIRA polyclonal antibody was used as a negative control.

cDNA sequence is incomplete. Interestingly, a conserved, in-frame stop codon is found near the beginning of intron 6, and retention of this intron would prevent translation of the larger protein in both mouse and human cells, perhaps yielding a smaller protein with a size corresponding to that previously predicted for hsGCN5.

To investigate the possibility of alternative (or incomplete) splicing of mouse and human *GCN5* transcripts, we performed RT-PCR on total RNA isolated from human HeLa cells, human hepatoma cells, mouse kidney, mouse ovary, and a 13.5-dpc mouse embryo. All RNAs were treated with RNase-free DNase I before RT-PCR to remove any genomic DNA from the samples. An *mmGCN5* genomic DNA clone was used in a separate reaction, as a positive control for the presence of the intron sequences. Two primers corresponding to conserved sequences in exons 6 and 8, which flank introns 6 and 7 (Fig. 3A and B), were used for the amplification. The RT-PCR products were separated on an agarose gel, transferred to a membrane, and then probed sequentially with *mmGCN5* cDNA sequences or intron 6 sequences.

A predominant RT-PCR product of a size corresponding to the spliced cDNA (lacking the intron) was amplified from mouse embryonic, kidney, and ovarian RNAs (lower band in Fig. 3B). As expected, this product was significantly smaller (126 bp) than the amplification product from the genomic DNA (about 1 kb), which contains introns 6 and 7. This small product hybridized to the *mmGCN5* cDNA sequences but not to the intron 6 probe, consistent with the removal of these intronic sequences by splicing. In contrast, two less abundant, closely spaced bands were detected by both the cDNA and the intron 6 probes. An intron 7 probe hybridized only to the genomic DNA but failed to detect any of the RT-PCR products (data not shown), suggesting that intron 7 had been removed in all of the transcripts. Sequencing of the larger, closely spaced RT-PCR products revealed that they represent two alternatively spliced variants of *mmGCN5* (Fig. 3C). Both of these variants retained intron 6, but one also contained a novel 25-bp exon (exon 7) located between introns 6 and 7. Intron 7 was removed from both of these alternatively spliced products, bringing the stop codons in intron 6 to a position just upstream of the ATG sequence corresponding to the previously predicted translation start site of hsGCN5. Together these data indicate that the predominant form of the mouse cDNA is completely spliced, lacks these stop codons, and therefore is predicted to encode the longer version of GCN5. However, the two minor RT-PCR products that we observed might encode shorter GCN5 proteins, consisting of the amino-terminal, P/CAF-like domain in isolation or of the C-terminal domain, which is most similar to yeast GCN5.

RT-PCR of total RNA from human cells revealed a similar mixture of completely and incompletely spliced RNAs. For example, two RT-PCR products were generated from the human HeLa cell and hepatoma cell RNAs. The size of the more abundant, smaller product again is consistent with a spliced cDNA lacking sequences homologous to the mouse intron 6 and exon 7, and this product hybridizes only to cDNA sequences. The less abundant, larger product hybridizes to both intron and exon sequences (Fig. 3B, middle panel). We suggest that the longer product likely corresponds to the *hsGCN5* cDNA sequences previously reported, whereas the more prevalent, shorter form represents a spliced product predicted to encode a longer protein analogous to that encoded by the mouse cDNA isolated as described above.

Long GCN5 proteins are present in both human and mouse cells. To identify the size of the native mammalian GCN5 protein(s), total cell extracts prepared from a 12.5-dpc mouse embryo or human HeLa cells were probed with a polyclonal serum raised against the previously described hsGCN5 (generously provided by Shelley Berger, Wistar Institute). The hsGCN5-specific antiserum detected a 98-kDa protein in the HeLa cell nuclear extracts, consistent with the predicted size of the full-length GCN5 protein containing the extended amino-terminal region (Fig. 4A, left panel). To ensure that this band corresponded to mmGCN5 and that the hsGCN5 antibody did

not cross-react with P/CAF, we compared the relative signals obtained with the hsGCN5 antibody and a P/CAF antibody (generously provided by Yoshihiro Nakatani, National Institutes of Health) with extracts from U2OS cells or HeLa cells. The P/CAF antibody recognized a single band in the U20S extract, consistent with previous reports that P/CAF is well expressed in these cells (41), and in the HeLa cell nuclear extract. The hsGCN5 antibody, however, did not recognize any proteins of a similar size in either extract but did recognize a prominent band of ~98 kDa in the HeLa cell nuclear extract. Therefore, the hsGCN5 antibody does not appear to cross-react significantly with PCAF, and we conclude that the 98-kDa protein recognized by this antibody in HeLa cell extracts is GCN5.

The hsGCN5 antibody also recognized a faint 60-kDa band (lower arrow in right panel of Fig. 4A) in the HeLa cell extracts, close to the predicted size of the shorter GCN5 protein described previously (38) and above. Thus, both the long and short forms of GCN5 appear to be expressed in these cells, but the longer form appears to be predominant. Interestingly, the long form of GCN5 was the only form detected in mouse embryo extracts. The expression of GCN5 protein in the embryonic extracts is consistent with high levels of GCN5-specific RNA detected in these tissues (see Fig. 5). Moreover, since only very low levels of P/CAF RNA were detected at this (or any) stage of mouse embryogenesis (data not shown and see Fig. 5), these data further support our conclusion that the hsGCN5 antibody recognizes mmGCN5 rather than mmP/CAF. Neither the long nor the short form of GCN5 was detected by control, preimmune serum in either the mouse or human extracts (data not shown).

We also used the anti-hsGCN5 serum to immunoprecipitate GCN5 proteins from the mouse embryo extract. Precipitated proteins were then detected by Western blotting with the same serum. Again, a 98-kDa protein was detected by the hsGCN5 antibody but not by a control rabbit serum (Fig. 4B). Unfortunately, the shorter form of GCN5, if it was present, would comigrate with the immunoglobulin G band and thus could not be detected by this approach. Nevertheless, these experiments confirm the presence of the longer GCN5 protein in mouse embryos.

Cloning of *mmP/CAF*. A second *GCN5*-related cDNA clone that contained a high degree of similarity to *hsP/CAF* was isolated in our screen of the mouse cDNA library. Since all initial clones appeared to be incomplete, containing an 867-bp fragment of the cDNA (relative to the human sequence), a second library was screened by using GeneTrapper technology. Multiple full-length cDNAs containing an open reading frame predicted to encode 813 amino acids were obtained. This open reading frame exhibited 93% identity to the *hsP/CAF* cDNA sequence but only 75% identity to the reported *hsGCN5* cDNA sequence (41). We therefore designated this clone *mmP/CAF*. Both the mmGCN5 and the mmP/CAF sequences possess predicted catalytic domains and bromodomains identified in a number of recently identified histone acetyltransferases, including several highly conserved amino acids near the putative catalytic center (Fig. 1).

Using a fragment from the 5′ region of the *mmP/CAF* cDNA as a probe, we identified multiple clones from a library of mouse genomic sequences that contained *P/CAF* sequences. Four of these contained different portions of the cDNA sequence. These clones indicate that in contrast to the *mmGCN5* gene, which contains small introns (a few hundred base pairs each), the *mmP/CAF* gene contains very large introns (16 to 20 kb). Because of these large introns, we have not completed cloning of *mmP/CAF* genomic sequences.

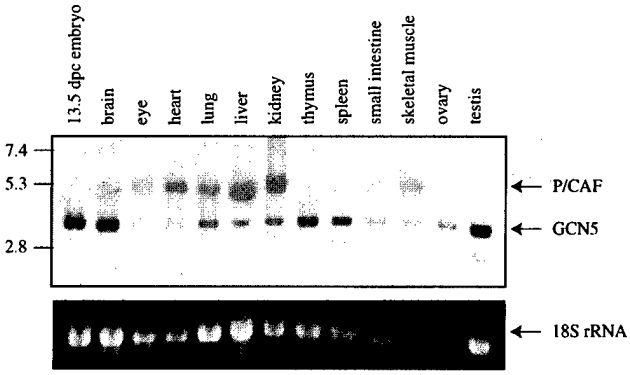

FIG. 5. Ubiquitous and complementary expression of mmGCN5 and mmP/CAF. (Top panel) Total RNA was isolated from various mouse tissues and embryos as indicated. Northern blot hybridization was performed with a mixture of *mmGCN5* and *mmP/CAF* cDNA probes. Two transcripts were detected and are indicated by arrows on the right. The identities of the transcripts were confirmed by Northern blot hybridization with single *GCN5* or *P/CAF* probes (data not shown). Positions of RNA molecular size standards (in kilobases) are shown on the left. (Bottom panel) Ethidium bromide-stained gel showing 18S rRNAs.

Interestingly, several clones identified in our genomic screens apparently contain a *P/CAF* pseudogene. No intronic sequences are present in these clones, and several base substitutions, relative to the cDNA sequence, are scattered throughout the predicted coding region of the pseudogene. RT-PCR analysis indicates that the pseudogene is not expressed in several mouse tissues examined, including brain, eye, heart, lung, liver, kidney, thymus, spleen, fat, diaphragm, small intestine, ovary, testis, or a 13.5-dpc embryo (data not shown).

Ubiquitous but complementary expression of *mmGCN5* and *mmP/CAF*. To examine and compare the expression of *mmGCN5* and *mmP/CAF*, total RNA was extracted from various mouse tissues, subjected to denaturing electrophoresis, transferred to a membrane, and then probed with *mmGCN5*- or *mmP/CAF*-specific sequences.

A single transcript of 3.3 kb was detected in all tissues with the *GCN5* probe, consistent with size of the cDNA clone we isolated. Similarly, a single, ubiquitous transcript was detected with the *P/CAF* probe, and the size of this RNA, 4.4 kb, is similar to that of the *P/CAF* cDNA that we isolated. Interestingly, the *P/CAF* RNA always exhibited a broader banding pattern than did the *GCN5* RNA. These two RNAs were clearly distinguished from one another when probed on the same blot, and a differential pattern of expression was detected (Fig. 5). For example, the ratio of *mmGCN5* to *mmP/CAF* expression is higher in brain, thymus, spleen, testis, and 13.5-dpc embryonic tissue, while this ratio is much lower in heart, liver, kidney, and skeletal muscle. Western blot analysis of GCN5 protein levels (with the polyclonal antiserum to hsGCN5 described above) in various mouse tissues confirmed the general pattern of expression indicated by this RNA analysis (data not shown).

Chromosomal locations of the *mmGCN5* and *mmP/CAF* genes. The chromosomal location of the *mmGCN5* gene was mapped by standard linkage analysis with the Jackson Laboratory interspecific backcross panel (C57BL/6Jei × SPRET/Ei)F_1 × SPRET/Ei, also known as Jackson BSS (33). *mmGCN5* mapped cleanly to a distal region on chromosome 11 and cosegregated tightly with *BRCA1*, as well as with a number of other genes previously mapped to that locus (data not shown, but raw data from the Jackson Laboratory are available at http://www.jax.org/resources/documents/cmdata).

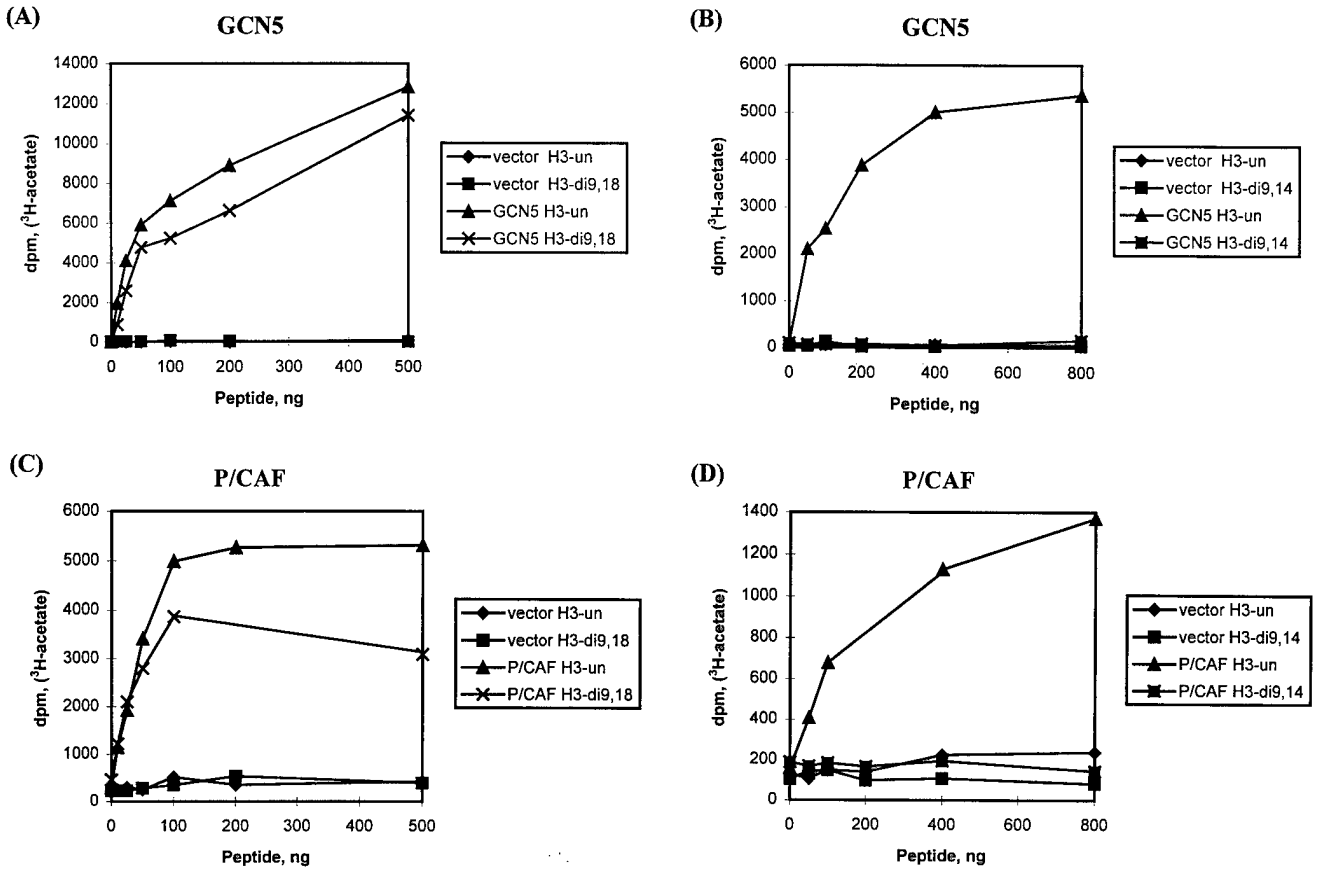

FIG. 6. Acetylation of histone H3 synthetic peptides by mmGCN5 and mmP/CAF. (A and B) Results of acetyltransferase assays with recombinant full-length mmGCN5 and synthetic peptides corresponding to the amino-terminal tail of histone H3. (C and D) Results of peptide assays with recombinant mmP/CAF. Peptides were either unacetylated (un) or synthesized with acetyl-lysine residues at either K9 and K18 (di9,18) or K9 and K14 (di9,14) in H3. Vector indicates assay of a control extract, made from bacteria transformed by the recombinant vector without an acetyltransferase insert, subjected to the His tag purification procedure.

Interestingly, the *hsGCN5* gene was recently mapped by fluorescent in situ hybridization analysis to a syntenic region of human chromosome 17 (9) and was also found to cosegregate with human *BRCA1*.

The location of *mmP/CAF* was mapped in a similar fashion, using the same backcross panel. In this case we used a probe specific for intronic sequences to ensure that we mapped the authentic *mmP/CAF* gene and not the *P/CAF* pseudogene. This analysis indicated that *mmP/CAF* is located 32 centimorgans from the centromere of mouse chromosome 17 and that it cosegregates with the DNA marker D17Bir8 (see www address above).

***mmGCN5* encodes a histone acetyltransferase with substrate specificity similar to that of P/CAF.** The high degree of homology between the mouse, human, and yeast GCN5 proteins strongly predicts that mmGCN5 and mmP/CAF will exhibit histone acetyltransferase activity. We confirmed this initially by examining the activities of the isolated, conserved acetylase domains of mmGCN5 and mmP/CAF, expressed as recombinant proteins in *Escherichia coli*. As expected, this domain of mmGCN5 was quite active as a histone acetylase, and it preferentially acetylated free (nonnucleosomal) histone H3, and to a lesser degree H4, as does yeast Gcn5p (23) and the previously reported form of the hsGCN5 protein (41). Full-length mmGCN5 and mmP/CAF recombinant proteins (also expressed in bacteria) exhibited this same substrate specificity towards free histones (Fig. 6 and data not shown).

To determine which residues of histone H3 were acetylated by mmGCN5, we performed assays with synthetic peptides corresponding to the amino-terminal tail of this histone. As expected, we found that the full-length GCN5 protein efficiently acetylated peptides corresponding to the first 20 amino acids of histone H3 (Fig. 6A and B). This domain alone, then, is sufficient for binding to the enzyme and subsequent catalysis. However, mmGCN5 could not acetylate a peptide that contained acetyl-lysine moieties at positions 9 and 14 (Fig. 6B), suggesting that one or both of these lysines may be a target site for mmGCN5. In contrast, mmGCN5 readily acetylated a peptide containing acetyl-lysine moieties at positions 9 and 18 (Fig. 6A). Taken together, these data suggest that K14 is the preferred acetylation site in H3 for mmGCN5. Similar assays performed with H4 peptides indicate that K8 is the preferred site of acetylation in H4 (data not shown). These results are consistent with the site specificity determined for recombinant yeast Gcn5p, which was confirmed by protein sequencing of acetylated histones (23). Importantly, these results indicate that the extended amino-terminal domain of mmGCN5 does not change the histone or lysine residue specificity of the enzyme.

The specificity of mmP/CAF was also tested with the peptide substrates. In all respects, mmP/CAF exhibited a substrate specificity identical to that of mmGCN5 (Fig. 6C and D).

One striking difference between the previously reported, shorter form of recombinant hsGCN5 (or yeast Gcn5p) and

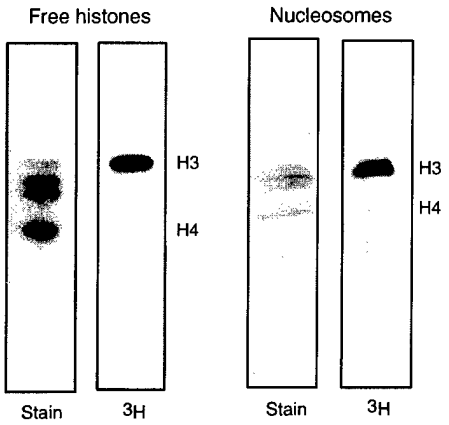

FIG. 7. Acetylation of nucleosomal histones by mmGCN5 and mmP/CAF. Acetyltransferase assays were performed with HeLa cell mononucleosomes or free histones as indicated, and an aliquot of each assay mixture was resolved on an SDS–22% polyacrylamide gel. Coomassie blue-stained gels and corresponding autoradiographs are shown. In both assays, histones H3 and H4 were acetylated by the recombinant full-length mmGCN5.

recombinant hsP/CAF was the ability of P/CAF to acetylate nucleosomal substrates (23, 41). Given the homology between the amino-terminal portions of P/CAF and mmGCN5, we asked whether the full-length recombinant mmGCN5 could also acetylate histones within a nucleosome. We found that mmGCN5, like hsP/CAF, can acetylate nucleosomal H3 and, to a lesser degree, H4 (Fig. 7). In agreement with previously reported results (23, 41), we also found that the short form of mmGCN5 or yeast Gcn5p was unable to acetylate nucleosomes (data not shown). These results suggest that one function of the amino-terminal domains of mammalian GCN5 and P/CAF may be to facilitate the recognition of chromatin templates.

mmGCN5 and mmP/CAF both interact with CBP and p300. hsP/CAF interacts with CBP and p300 (41). Given the similarity between mmGCN5 and mmP/CAF, we examined the abilities of both of these proteins to bind to CBP or p300 in vitro (Fig. 8).

Whole-cell lysates from bacteria expressing fragments of CBP fused to GST (fusion constructs were kindly provided by Y. Nakatani, National Institutes of Health) (41) were mixed with lysates from cells expressing the amino-terminal domain of mmP/CAF, the amino-terminal domain of mmGCN5, or the C-terminal domain of mmGCN5. The CBP fragments (A to F) spanned the ADA2 homology domain and extended into the transcriptional activation domain (41). A fragment of p300 (B′) homologous to the B fragment of CBP was also tested. GST fusion proteins were purified together with any interacting proteins by using glutathione-Sepharose, and the interacting proteins were identified by Western blotting with an antiserum specific for the six-histidine tag present in the recombinant mmP/CAF or mmGCN5 protein.

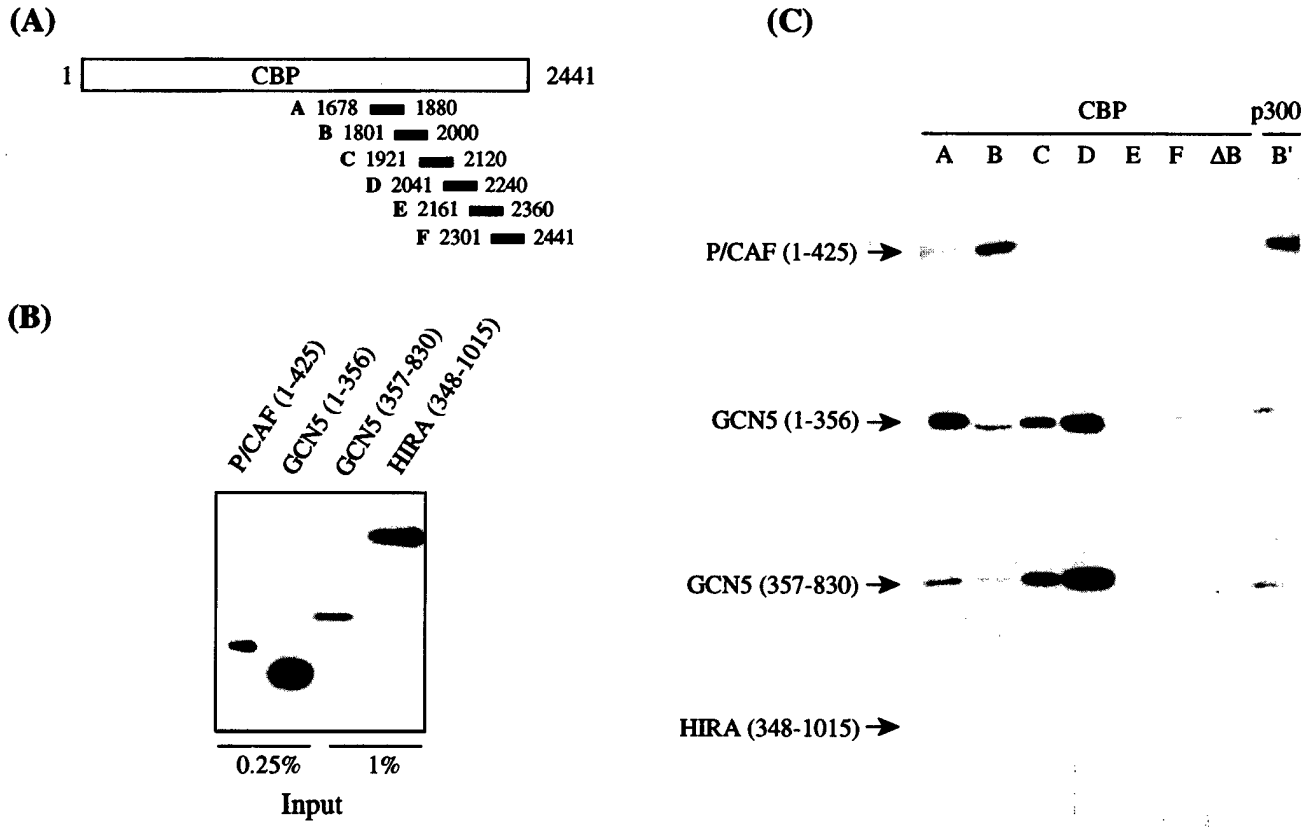

FIG. 8. mmGCN5 and mmP/CAF both interact with CBP and p300 in vitro. (A) Fragments of CBP fused to GST that were used for the interaction assays in panel C. These fragments span the region of homology to ADA2 and extend into the transactivation domain of CBP (41). (B) Recombinant, His-tagged proteins used in the interaction assays of panel C were resolved by SDS-polyacrylamide gel electrophoresis and probed with an antibody specific for the His tag. The amounts shown represent 0.25 or 1% of the protein used in the assay, as indicated. (C) GST-CBP or -p300 fusion proteins were mixed with crude bacterial lysates containing P/CAF, GCN5, or HIRA protein. Interacting proteins were recovered by using glutathione-Sepharose and detected on Western blots with the anti-His tag antibody. The p300 B′ fragment is homologous to the CBP B fragment, and the CBP ΔB fragment is missing residues 1801 to 1851 (41).

The amino-terminal domain of mmP/CAF selectively bound to fragments A and B of CBP and the corresponding B′ fragment of p300. In some experiments, we also observed binding to the D fragment, but we never observed binding to fragment C, E, or F. A deletion within the B fragment (ΔB) of CBP that removed residues 1801 to 1851 eliminated binding. This pattern of binding to the CBP/p300 fragments is extremely similar to that previously reported for hsP/CAF (41), as expected.

A recombinant form of hsGCN5, which lacked the amino-terminal domain reported here for mmGCN5, failed to bind CBP or p300 in previous experiments by Yang et al. (41). This form of hsGCN5 corresponds to the C-terminal region of mmGCN5. We therefore compared binding of the amino-terminal and the C-terminal halves of mmGCN5 to the GST-CBP and -p300 fragments. Surprisingly, we found that both of these mmGCN5 domains bound to CBP fragments A to D, with little or no binding to fragment E, fragment F, or the ΔB fragment. Both the amino-terminal and C-terminal regions of mmGCN5 also bound to the p300 B′ fragment. The amount of the GST fusion proteins recovered from the GST columns that did not exhibit binding to the GCN5 fragments was greater than or equal to that of the GST fusions that did exhibit binding (data not shown), so the absence of binding was not due to reduced amounts of the E, F, or ΔB fragment. In addition, the selective binding of the mmGCN5 peptides to CBP fragments A to D indicates that these interactions are not nonspecifically mediated by the GST moiety, since this moiety is also present in fragments E, F, and ΔB. The specificity of the interactions was further tested by using an unrelated protein, HIRA, which failed to bind to any of the GST-CBP or -p300 fragments. Thus, CBP fragments A to D do not exhibit general, nonspecific binding to random proteins. We conclude that mmGCN5 contains two distinct CBP/p300 interaction domains and that these domains interact with a broader region in CBP than does P/CAF. Importantly, our finding that mmGCN5 and mmP/CAF can both interact with CBP/p300 indicates that these proteins are very similar in function as well as in structure.

DISCUSSION

The recent identification of nuclear histone acetyltransferases has directly linked chromatin modification with transcriptional regulation (1, 5, 26, 29). We report here the cloning of *mmGCN5* and *mmP/CAF* sequences. We find that *mmGCN5* differs from yeast *GCN5* and the previously reported *hsGCN5* sequences in that it encodes a large N-terminal domain similar to that found in P/CAF. Our data indicate that hsGCN5 contains this extra domain as well. While this domain does not appear to affect the histone specificity of the acetyltransferase, it does afford the enzyme the ability to modify nucleosomal substrates in vitro.

In vivo, both the yeast and mammalian enzymes must interact with and modify nucleosomal histones. In yeast, this is accomplished by association of Gcn5p into high-molecular-weight protein complexes that can modify nucleosomes and that recognize additional histones (14). At least some of the Gcn5p-associated proteins are conserved in higher eukaryotes, and Gcn5-Ada complexes have been identified in human cells (7), further indicating that these enzymes serve similar functions across species. We scanned the yeast genome database to determine whether a protein homologous to the amino-terminal domains of mmGCN5 or mmP/CAF might exist that could be a component of the Gcn5p-containing complexes. However, we found no such homologs.

Interestingly, a single *GCN5*-related gene has been identified in *Drosophila*. This gene exhibits high similarity to mammalian *P/CAF* (34a) and encodes the extended N-terminal domain. Although this domain is apparently not needed in yeast, its functions are not restricted to mammals.

Our work indicates that multiple differentially spliced forms of *GCN5* transcripts coexist in both mouse and human cells, which may generate different isoforms of GCN5 proteins. Of course, we cannot rule out the possibility that the less abundant products represent incompletely spliced RNAs, but it is interesting that intron 6 and the stop codons therein are conserved between human and mouse. Since we detected transcripts containing intron 6 in both mouse and human tissues, we are intrigued by the possibility that shortened GCN5 proteins, containing either the N-terminal domain alone or the C-terminal domain alone, may provide an additional level of regulation of GCN5 functions. For example, we detected the full-length GCN5 protein in mouse embryo extracts and some human cells, but we detected a shorter, less abundant protein in HeLa cells in addition to the full-length protein. It will be especially interesting to determine whether various forms of GCN5 proteins are differentially regulated in different cell types or at different developmental stages.

The long form of mmGCN5 is very similar to mmP/CAF in structure, in acetyltransferase activity and substrate specificity, and in interactions with CBP/p300. Additional experiments are needed to determine whether these two proteins are functionally redundant in vivo. Even if GCN5 and P/CAF perform the same functions, they might be utilized at different developmental stages or in different cell types or tissues. The similarity between these proteins is somewhat reminiscent of that between CBP and p300. These two proteins also appear to be functionally equivalent in vitro, but mutations in p300 and CBP cause different phenotypes (27, 30), indicating that the proteins are not functionally redundant in vivo. It will be interesting to determine whether the same is true for mmGCN5 and mmP/CAF.

Several histone acetyltransferases, including p300/CBP and P/CAF, have been implicated in growth control and tumorigenesis (30, 32, 41). p300/CBP physically interacts with the tumor suppressor p53 and potentiates sequence-specific DNA binding and transactivation by p53 through acetylation of its C-terminal domain (15). Moreover, mutations in p300 have been found in certain colorectal and gastric cancers (27). CBP mutations are also involved in the etiology of certain acute myeloid leukemias and Rubinstein-Taybi syndrome (30), a developmental disorder with a high incidence of neoplasms. In addition, P/CAF counteracts the transforming activity elicited by oncoprotein E1A, and overexpression of P/CAF has been shown to inhibit cell cycle progression (41). Therefore, histone acetyltransferases have been postulated to be negative regulators of cell growth and, possibly, tumor suppressors. We (this study) and others (9) have found that *GCN5* cosegregates with the tumor suppressor *BRCA1* gene (1-centimorgan interval) in a highly syntenic region in mouse (chromosome 11) and human (chromosome 17). Interestingly, loss of heterozygosity on human chromosome 17 is a frequent genetic alteration in sporadic breast and ovarian cancers, where mutations in *BRCA1* and *BRCA2* are rarely found (28, 35). Indeed, a novel tumor suppressor gene involved in these cancers has been postulated to be located adjacent to the *BRCA1* locus (28, 35). *GCN5* may provide an attractive candidate for this novel tumor suppressor. The isolation and characterization of *mmGCN5* and *mmP/CAF* reported here should facilitate further study of the roles of these genes and of histone acetylation in normal mammalian development, as well as in abnormal events leading to tumorigenesis.

ACKNOWLEDGMENTS

We thank Jerry Workman and Patrick Grant for the kind gift of HeLa cell mononucleosomes and histones. We thank David Allis for the gift of H3 amino-terminal peptides, and we thank E. Smith and D. Allis for the gift of oligomers for PCR and for sharing results prior to publication. We also thank Shelley Berger for antiserum specific for hsGCN5, Yongshen Ren for the gift of HeLa cell nuclear extracts, and Yoshihiro Nakatani for the GST-CBP and GST-p300 fusion constructs and hsP/CAF antibodies. Some DNA sequencing was performed by the UTMDACC Sequencing Core Facility. We are grateful to Lucy Rowe and Mary Barter at the Jackson Laboratory for their assistance in the mouse chromosome mapping analysis. We thank Karen Hensley for help in preparation of some graphics and Aurora Diaz for help in preparing the manuscript.

W.X. is supported by a Rosalie B. Hite Fellowship, and D.G.E. is supported by a Theodore Law UCF Scientific Fund Fellowship. This work was supported by grants to S.Y.R. from the Robert A. Welch Foundation, the USARMC, and the Breast Cancer Research Center at UTMDACC.

The first two authors contributed equally to this work.

REFERENCES

1. **Bannister, A. J., and T. Kouzarides.** 1996. The CBP co-activator is a histone acetyltransferase. Nature **384:**641–643.
2. **Barlev, N., R. Candau, L. Wang, P. Darpino, N. Silverman, and S. Berger.** 1995. Characterization of physical interactions of the putative transcriptional adaptor, ADA2, with acidic activation domains and TATA binding protein. J. Biol. Chem. **270:**19337–19344.
3. **Berger, S. L., B. Pina, N. Silverman, G. A. Marcus, J. Agapite, J. L. Regier, S. J. Triezenberg, and L. Guarente.** 1992. Genetic isolation of ADA2: a potential transcriptional adaptor required for function of certain acidic activation domains. Cell **70:**251–265.
4. **Brownell, J. E., and C. D. Allis.** 1995. An activity gel assay detects a single, catalytically active histone acetyltransferase subunit in Tetrahymena macronuclei. Proc. Natl. Acad. Sci. USA **92:**6364–6368.
5. **Brownell, J. E., J. Zhou, T. Ranalli, R. Kobayashi, D. G. Edmondson, S. Y. Roth, and C. D. Allis.** 1996. Tetrahymena histone acetyltransferase A: a homolog to yeast Gcn5p linking histone acetylation to gene activation. Cell **84:**843–851.
6. **Candau, R., and S. L. Berger.** 1996. Structural and functional analysis of yeast putative adaptors: evidence for an adaptor complex in vivo. J. Biol. Chem. **271:**5237–5243.
7. **Candau, R., P. A. Moore, L. Wang, N. Barlev, C. Y. Ying, C. A. Rosen, and S. L. Berger.** 1996. Identification of functionally conserved human homologs of the yeast adapters ADA2 and GCN5. Mol. Cell. Biol. **16:**593–602.
8. **Candau, R., J. Zhou, C. D. Allis, and S. L. Berger.** 1997. Histone acetyltransferase activity and interaction with ADA2 are critical for GCN5 function in vivo. EMBO J. **16:**555–565.
9. **Carter, K. C., L. Wang, B. K. Shell, I. Zamir, S. L. Berger, and P. A. Moore.** 1997. The human transcriptional adaptor genes TADA2L and GCN5L2 colocalize to chromosome 17q12-q21 and display a similar tissue expression pattern. Genomics **40:**497–500.
10. **Chomczynski, P., and N. Sacchi.** 1987. Single-step method of RNA isolation by acid guanidinium thiocyanate-phenol-chloroform extraction. Anal. Biochem. **162:**156–159.
11. **Edmondson, D. G., and E. N. Olson.** 1989. A gene with homology to the myc similarity region of MyoD1 is expressed during myogenesis and is sufficient to activate the muscle differentiation program. Genes Dev. **3:**628–640.
12. **Edmondson, D. G., and S. Y. Roth.** 1996. Chromatin and transcription. FASEB J. **10:**1173–1182.
13. **Georgakopoulos, T., and G. Thireos.** 1992. Two distinct yeast transcriptional activators require the function of the GCN5 protein to promote normal levels of transcription. EMBO J. **11:**4145–4152.
14. **Grant, P. A., L. Duggan, J. Cote, S. Roberts, J. E. Brownell, R. Candau, R. Ohba, T. Owen-Hughes, C. D. Allis, F. Winston, S. L. Berger, and J. L. Workman.** 1997. Yeast GCN5 functions in two multisubunit complexes to acetylate nucleosomal histones: characterization of an ADA complex and the SAGA (SPT/ADA) complex. Genes Dev. **11:**1640–1650.
15. **Gu, W., and R. G. Roeder.** 1997. Activation of p53 sequence-specific DNA binding by acetylation of the p53 C-terminal domain. Cell **90:**595–606.
16. **Hansen, J. C.** 1997. The core histone amino-termini: combinatorial interaction domains that link chromatin structure with function. Chem Tracts Biochem. Mol. Biol. **10:**56–69.
17. **Haynes, S. R., C. Dollard, F. Winston, S. Beck, J. Trowsdale, and I. B. Dawid.** 1992. The bromodomain: a conserved sequence found in human, Drosophila and yeast proteins. Nucleic Acids Res. **20:**2603.
18. **Horiuchi, J., N. Silverman, G. A. Marcus, and L. Guarente.** 1995. ADA3, a putative transcriptional adaptor, consists of two separable domains and interacts with ADA2 and GCN5 in a trimeric complex. Mol. Cell. Biol. **15:**1203–1209.
19. **Jeanmougin, F., J.-M. Wurtz, B. Le Douarin, P. Chambon, and R. Losson.** 1997. The bromodomain revisited. Trends Biochem. Sci. **22:**151–153.
20. **Korzus, E., J. Torchia, D. W. Rose, L. Xu, R. Kurokawa, E. M. McInerney, T.-M. Mullen, C. K. Glass, and M. G. Rosenfeld.** 1998. Transcription factor-specific requirements for co-activators and their acetyltransferase functions. Science **279:**703–707.
21. **Kozak, M.** 1991. An analysis of vertebrate mRNA sequences: intimations of translational control. J. Cell Biol. **115:**887–904.
22. **Kozak, M.** 1991. Structural features in eukaryotic mRNAs that modulate the initiation of translation. J. Biol. Chem. **266:**19867–19870.
23. **Kuo, M. H., J. E. Brownell, R. E. Sobel, T. A. Ranalli, R. G. Cook, D. G. Edmondson, S. Y. Roth, and C. D. Allis.** 1996. Transcription-linked acetylation by Gcn5p of histones H3 and H4 at specific lysines. Nature **383:**269–272.
24. **Marcus, G., N. Silverman, S. Berger, J. Horiuchi, and L. Guarente.** 1994. Functional similarity and physical association between GCN5 and ADA2, putative transcriptional adaptors. EMBO J. **13:**4807–4815.
25. **Marcus, G. A., J. Horiuchi, N. Silverman, and L. Guarente.** 1996. ADA5/SPT20 links the ADA and SPT genes, which are involved in yeast transcription. Mol. Cell. Biol. **16:**3197–3205.
26. **Mizzen, C. A., X. J. Yang, T. Kokubo, J. E. Brownell, A. J. Bannister, T. Owen-Hughes, J. Workman, L. Wang, S. L. Berger, T. Kouzarides, Y. Nakatani, and C. D. Allis.** 1996. The TAF(II)250 subunit of TFIID has histone acetyltransferase activity. Cell **87:**1261–1270.
27. **Muraoka, M., M. Konishi, R. Kikuchi-Yanoshita, K. Tanaka, N. Shitara, J. Chong, T. Iwama, and M. Miyaki.** 1996. p300 gene alterations in colorectal and gastric carcinomas. Oncogene **12:**1565–1569.
28. **Niederacher, D., F. Picard, C. V. Roeyen, H. An, H. G. Bender, and M. W. Beckmann.** 1997. Patterns of allelic loss on chromosome 17 in sporadic beast carcinomas detected by fluorescent-labeled microsatellite analysis. Genes Chromosomes Cancer **18:**181–192.
29. **Ogryzko, V. V., R. L. Schlitz, V. Russanova, B. H. Howard, and Y. Nakatani.** 1996. The transcriptional coactivators p300 and CBP are histone acetyltransferases. Cell **87:**953–959.
30. **Petrij, F., R. H. Giles, H. G. Dauwerse, J. J. Saris, R. C. M. Hennekam, M. Masuno, N. Tommerup, G.-J. B. van Ommen, R. H. Goodman, D. J. M. Peters, and M. H. Breuning.** 1995. Rubinstein-Taybi syndrome caused by mutations in the transcriptional co-activator CBP. Nature **376:**348–351.
31. **Roberts, S. M., and F. Winston.** 1996. *SPT20/ADA5* encodes a novel protein functionally related to the TATA-binding protein and important for transcription in *Saccharomyces cerevisiae*. Mol. Cell. Biol. **16:**3206–3213.
32. **Roth, S. Y.** 1996. Something about silencing. Nat. Genet. **14:**3–4.
33. **Rowe, L. B., J. H. Nadeau, R. Turner, W. N. Frankel, V. A. Letts, J. T. Eppig, M. S. H. Ko, S. J. Thurston, and E. H. Birkenmeier.** 1994. Maps from two interspecific backcross DNA panels available as a community genetic mapping resource. Mamm. Genome **5:**253–274.
34. **Silverman, N., J. Agapite, and L. Guarente.** 1994. Yeast ADA2 binds to the VP16 protein activation domain and activates transcription. Proc. Natl. Acad. Sci. USA **91:**11665–11668.

34a. **Smith, E., and D. Allis.** Personal communication.

35. **Tangir, J., M. G. Muto, R. S. Berkowitz, W. R. Welch, D. A. Bell, and S. C. Mok.** 1996. A 400 kb novel deletion unit centromeric to the BRCA1 gene in sporadic epithelial ovarian cancer. Oncogene **12:**735–740.
36. **Turner, B. M.** 1991. Histone acetylation and control of gene expression. J. Cell Sci. **99:**13–20.
37. **van Holde, K. E.** 1989. Chromatin. Springer-Verlag, New York, N.Y.
38. **Wang, L., C. Mizzen, C. Ying, R. Candau, N. Barlev, J. Brownell, C. D. Allis, and S. L. Berger.** 1997. Histone acetyltransferase activity is conserved between yeast and human GCN5 and is required for complementation of growth and transcriptional activation. Mol. Cell. Biol. **17:**519–527.
39. **Wolffe, A.** 1992. Chromatin structure and function. Academic Press, London, United Kingdom.
40. **Wolffe, A. P., and D. Pruss.** 1996. Targeting chromatin disruption: transcription regulators that acetylate histones. Cell **84:**817–819.
41. **Yang, X.-J., V. V. Ogryzko, J.-I. Nishikawa, B. H. Howard, and Y. Nakatani.** 1996. A p300/CBP associated factor that competes with the adenoviral oncoprotein E1A. Nature **382:**319–324.

Loss of GCN5 Leads to Increased Apoptosis and Mesodermal Defects During Mouse Development

Wanting Xu*, Diane G. Edmondson*, Yvonne A. Evrard*, Maki Wakamiya[+],

Richard R. Behringer[+], & Sharon Y. Roth*

* Department of Biochemistry and Molecular Biology, [+]Department of Molecular Genetics,

University of Texas M.D. Anderson Cancer Center, Houston, Texas 77030, USA

Key words: acetyltransferase, chromatin, mesoderm, apoptosis, development

Histone acetyltransferases (HATs) are important in transcriptional regulation, but little is known about the role of these enzymes in developmental processes. Two mouse HATs, Gcn5 (Gcn512) and Pcaf, share similar sequences and enzymatic activities[1]. Both interact with p300/CBP (Ep300/Crebbp), two other HATs that integrate multiple signaling pathways[1]. Pcaf is thought to participate in many of the cellular processes regulated by p300/CBP[2-8], but Gcn5 functions are relatively understudied in mammalian cells. Here we show that *Pcaf* is dispensable in mice. In contrast, *Gcn5* null embryos die during embryogenesis. These embryos develop normally to 7.5 dpc but are severely growth retarded by 8.5 dpc and fail to form dorsal mesoderm lineages, including chordamesoderm and paraxial mesoderm. Differentiation of extraembryonic and cardiac mesoderm appears unaffected. Strikingly, loss of the dorsal mesoderm lineages is due to a high incidence of apoptosis in the *Gcn5* mutants that begins before the onset of morphological abnormality. Embryos null for both *Gcn5* and *Pcaf* show even more severe defects, indicating that these HATs have overlapping functions during embryogenesis. Our studies are the first to demonstrate that specific acetyltransferases are required for cell survival and mesoderm formation during mammalian development.

Mouse *Gcn5* and *Pcaf* are expressed ubiquitously, but in complementary amounts, in different adult mouse tissues[1]. During embryogenesis, *Gcn5* is expressed uniformly throughout the embryo from 7.5-9.0 days post coitum (dpc), except in the distal allantois and developing heart (Fig. 1*c*). *Gcn5* expression is down-regulated after 16.5 dpc (Fig. 1*a*) but is later up-regulated in specific adult tissues[1]. In contrast, *Pcaf* expression is low during embryogenesis and becomes up-regulated in some adult tissues including heart and skeletal muscle (Fig. 1*b*).

To decipher the roles of these enzymes in mammalian development, we generated mice lacking *Pcaf* or *Gcn5* (Figs. 2*a*, *b*, and 3*a-c*). Mice null for *Pcaf* are viable and fertile with no obvious abnormal phenotype. In addition, we observed no apparent up-regulation of either *Gcn5* mRNA (Fig. 2*c*) or protein

levels (data not shown). Mice heterozygous for the *Gcn5* null allele were obtained at the expected frequency and appeared normal. *Gcn5* null mice appeared normal and exhibited Mendelian segregation at 7.5 dpc (data not shown). However by 8.5 dpc, *Gcn5* null embryos were growth retarded and died by 10.5 dpc. Histological analysis indicated that *Gcn5* null embryos lacked specific mesodermal derived structures, such as somites, and rarely formed a recognizable notochord or neural tube (Fig. 4*a-l*). An ectopic structure in the exocoelomic cavity projects from the anterior end of null embryos (Fig. 3*d*, 4*m-u*). Histologically this structure resembles ectodermal cells (Fig. 4*g-i*), but it does not express neural (*Otx2*, *En1*, and *Hes5*; data not shown) or mesodermal lineage markers (see below).

To determine which mesodermal derivatives are missing in the *Gcn5* null embryos, we examined the expression of mesoderm lineage markers (Fig. 4*m-u*). *T*[9](*Brachyury*) and *Fgf8*[10] were detected in the mutant embryos at 8.25 dpc (Fig. 4*m-n*) indicating that the primitive streak forms. However, we observed deficits in the expression of *Tcf15*[11](*paraxis*) and *Dll1*[12] (*Delta-like 1 homolog)* in 8.5 dpc mutants (Fig. 4*o*, *q*), indicating that paraxial mesoderm is disrupted. Similarly, no expression of *Shh*[13] (*Sonic hedgehog*) or *Foxa2*[14,15](*Hnf-3b*) was observed along the anterior midline of 8.5 dpc *Gcn5* null embryos (Fig. 4*r*, *s*) indicating defective notochord formation. *Foxa2* expression was detected in the distal tip and the anterior lateral area of the mutant embryos, in the definitive endoderm and node. *Twist* expression was detected in the allantois of the *Gcn5* mutants but was barely detectable in embryonic tissues (Fig. 4*t*), suggesting that head mesenchyme formation is compromised[16,17]. *Mef2c*, an early marker for cardiac mesoderm[18], was expressed normally in the *Gcn5* mutants at 8.0 (Fig. 4*u*). This result is consistent with our observation that the *Gcn5* mutant embryos have heartbeats at 10.5 dpc and suggests that cardiac mesoderm formation is unaffected in these mutants. Together, these results indicate that mesoderm is formed in the *Gcn5* null embryos, but paraxial mesoderm, chordamesoderm and head mesenchyme do not develop normally.

The lineage-specific defects in mesoderm formation might arise from a lack of initial mesoderm specification. *Tcf15* is expressed as early as 7.5 dpc in wild type embryos so we re-examined *Tcf15* expression at this stage in the mutant. *Tcf15* expression was observed between 7.5-8.0 dpc (Fig. 4*p*), indicating that paraxial mesoderm is specified but not maintained in the absence of *Gcn5*. Similarly, *Shh* was expressed at 7.5 dpc, indicating specification and subsequent loss of chordamesoderm (data not shown).

Loss of mesodermal derivatives could be due to a failure of proliferation or to increased cell death. To distinguish between these two possibilities, we examined *Gcn5* mutants for expression of Proliferating Cell Nuclear Antigen (PCNA) and by TUNEL assay. We detected equal or higher amounts of PCNA in *Gcn5* mutants at 8.5 dpc compared to wild type embryos at 7.5 or 8.5 dpc, indicating that cell proliferation is not affected by *Gcn5* loss (data not shown). However, TUNEL assays reveal a strikingly high degree of apoptosis occurs in the mutants (Fig. 5*c-d*) at 7.5 dpc. Apoptotic cells are rarely found in 7.5 dpc wild type embryos (Fig. 5*a-b*). At 8.5 dpc, more than 25% of cells (Fig. 5*f*) are undergoing apoptosis in the mutants, whereas only about 1% of cells, mostly clustered in the midline of the neural tube, are apoptotic in wild type embryos (Fig. 5*e*). Increased cell death in the mutants is restricted to the embryonic ectoderm and mesoderm (Fig. 5*c*, *d* and *g*). Since it occurs before morphological defects are apparent, this increased cell death is likely responsible for the disappearance of dorsal mesoderm lineages in *Gcn5* mutants. Importantly, the increase in apoptosis does not reflect a general failure in transcription since *Tcf15* and other markers are expressed at 7.5 dpc in the *Gcn5* mutants.

Lastly, we generated mice harboring compound mutations for *Gcn5* and *Pcaf*. Mice heterozygous for *Gcn5* and null for *Pcaf* are morphologically normal. However, mice null for both HATs die around 7.5 dpc, several days earlier than the *Gcn5* mutants. Double mutants are severely retarded, and some yolk sacs are filled with blood (Fig. 6*a*). These embryos are observed at Mendelian ratios at 7.5 dpc, but are no longer found after 8.5 dpc. At 6.5 dpc, double null embryos are

developmentally retarded and appear arrested at the egg cylinder stage with severely disorganized embryonic ectoderm and visceral endoderm (Fig. 6*b-c*). Since the combined loss of *Pcaf* and *Gcn5* leads to more severe defects than observed for loss of *Gcn5* alone, *Gcn5* and *Pcaf* must share overlapping functions prior to 6.5 dpc.

Our studies yield several important conclusions. First, although Pcaf physically interacts with CBP and p300[1,6], the lack of a phenotype for the *Pcaf* mutant mice demonstrates that Pcaf is not absolutely required for p300 or CBP functions[19]. Second, the absence of *Gcn5* results in loss of paraxial mesoderm, chordamesoderm, and head mesenchyme due to a dramatic increase in apoptosis. Lastly, although Gcn5 also physically interacts with p300/CBP[1], the phenotypes of mice lacking *p300* are substantially different[19] from those lacking *Gcn5*, suggesting that Gcn5 functions are unique and are not merely supplementary to those of p300/CBP. Rather, these different phenotypes indicate that individual HATs are required as cofactors for specific developmental processes.

Methods

***Pcaf* targeting.** We isolated a portion of the *Pcaf* gene by screening a mouse genomic library (Lambda FIXII, Stratagene). One clone (19.5 kb) consists of two exons, which are 127 bp and 146 bp in length and are located 249 and 376 bp downstream of the translation start site in the *Pcaf* coding sequence. The latter exon was targeted. An SV40 poly-adenylation sequence was inserted into the targeting vector between the 5' and 3' homology arms. Upon homologous recombination, the targeted exon was replaced by the poly-adenylation sequence and the *PGK Neo* cassette which would prematurely terminate the *Pcaf* transcript. The length of the targeted exon is not a multiple of three base pairs, so in the event that splicing skips the targeted exon, the resulted cDNA would be out of frame for the Pcaf protein. For genotyping, genomic DNA was digested with *Pst*I or *Xba*I, and probed with a 1.3 kb *Pst*I-*Xba*I fragment (5' probe) or a 0.65 kb *Bam*HI fragment (3' probe) respectively (Fig. 2).

***Gcn5* targeting.** *Gcn5* genomic sequence that covers the entire *Gcn5* coding region was isolated previously[1]. A 1.5 kb genomic fragment upstream of the translation start site was used as 5' homology arm. A 5.5 kb fragment was excised by *Xba*I and *Not*I to generate the 3' homology arm. In addition, a *LacZ* gene was inserted into the *Gcn5* locus, where its transcription was to be driven by the *Gcn5* regulatory sequences (Fig. 3). Homologous recombination replaced the *Gcn5* coding region with the *LacZ* gene and the *PGK-Neo* cassette. For genotyping, genomic DNA was digested with *Eco*RV and probed with a 0.6 kb *Apa*I fragment 5' to the 5' homology arm. Similarly, genomic DNA was digested with *Eco*RV and probed with a 0.5 kb PCR generated fragment 3' to the 3' homology arm. PCR primers used to generate the 3' probe are: 5'- AGTAGGTGGTATGGCTTCTCAG; 3'- CTAGAAGGCTCAGGA TACCATC.

Creation of *Pcaf* or *Gcn5* null mice. *Gcn5* and *Pcaf* targeting vectors were linearized and electroporated separately into 129/SvEv derived ES cells AB1, originally generated by Dr. A Bradley (Baylor College of Medicine). G418 and FIAU double resistant cells were genotyped by Southern blot analyses using *Gcn5* or *Pcaf* probes described above. Correctly targeted ES cells were injected into 3.5 dpc C57BL/6J (Jackson Lab) blastocysts. Male chimeras were mated with wildtype C57BL/6J females. Germline transmission of the mutant allele was determined by Southern blot analysis of tail genomic DNA using the probes described above. Three out of four independent *Pcaf* targeted ES cell lines and two out of three independent *Gcn5* ES cell lines gave rise to germline transmission. Heterozygous mice were intercrossed to generate homozygous null mice. Embryos younger than 8.5 dpc were genotyped by PCR. Primers for *Gcn5*: 5' - AACCTGACCCTGGAGGATGCCAAG; 3' - GTGACGGCACAGAAGACGATTTCC. Primers for *Pcaf*: 5' – AAGCTGCTCACGTTTCTCACTT GG; 3'-GGGTAAGCTCTCACCTTGAATAGG. Primers for *Neo*: 5' – TCCTGCCGAGAAAGTATCC AT; 3' - AGGAAAGGACAGTGGGAGTGG. Primers for *LacZ*: 5' – GCATCGAGCTGGGTAATAA GGGTTGGCAAT; 3' - GACACCAGACCAACTGGTAATGGTAGCGAC.

Generation of *Pcaf* and *Gcn5* double mutants. *Gcn5* heterozygous mice were crossed with *Pcaf* heterozygotes to create mice doubly heterozygous for *Gcn5* and *Pcaf*. Double heterozygotes were mated with *Pcaf* null mice to produce mice that were heterozygous for *Gcn5* and null for *Pcaf*. Mice heterozygous for *Gcn5* and null for *Pcaf* were normal and intercrossed to generate mice that were doubly null for both genes.

RNA analysis. Total RNA from whole embryos or adult mouse tissues was isolated and electrophoresed on 1.5% agarose gels containing formaldehyde. RNA was transferred to GeneScreen Plus membrane (NEN Life Science) and hybridized with *Gcn5* and *Pcaf* cDNA probes as previously described[1].

Histological studies. Mouse embryos were fixed with 4% paraformaldehyde overnight at 4 °C, and dehydrated with graded alcohol. Embryos were cleared in xylene, incubated in 1:1 xylene/paraffin for 45 min at 65 °C, washed 3X with paraffin 30 min each at 65 °C, and embedded in paraffin. Sections were made at 7 μm and stained with hematoxylin and eosin according to standard procedure.

Whole-mount *in situ* hybridization. Whole mount in site hybridization of embryos was performed as described by Hogan et al. 1994[20]. Three or more embryos were used for each marker. The cDNAs used to generate probes used have been previously described[9,10,13-17]. The cDNAs used to generate probes for *Tcf15*[11] (*paraxis*) and *Mef2c*[18] were kindly provided by Dr. E. Olson.

TUNEL assay. TUNEL assay was performed on paraffin sections using the ApopTag Plus Peroxidase *In situ* Apoptosis Detection Kit purchased from Intergen according to the manufacturer's protocol.

1. Xu, W., Edmondson, D.G. & Roth, S.Y. Mammalian GCN5 and P/CAF acetyltransferases have homologous amino- terminal domains important for recognition of nucleosomal substrates. *Mol Cell Biol* **18**, 5659-69 (1998).

2. Blanco, J.C. *et al.* The histone acetylase PCAF is a nuclear receptor coactivator. *Genes Dev* **12**, 1638-51 (1998).

3. Liu, L. *et al.* p53 sites acetylated in vitro by Pcaf and p300 are acetylated in vivo in response to Dna damage. *Mol Cell Biol* **19**, 1202-9 (1999).

4. Puri, P.L. *et al.* Differential roles of p300 and PCAF acetyltransferases in muscle differentiation. *Mol Cell* **1**, 35-45 (1997).

5. Sakaguchi, K. *et al.* DNA damage activates p53 through a phosphorylation-acetylation cascade. *Genes Dev* **12**, 2831-41 (1998).

6. Yang, X.J., Ogryzko, V.V., Nishikawa, J., Howard, B.H. & Nakatani, Y. A p300/CBP-associated factor that competes with the adenoviral oncoprotein E1A. *Nature* **382**, 319-324 (1996).

7. Chakravarti, D. *et al.* A viral mechanism for inhibition of p300 and PCAF acetyltransferase activity. *Cell* **96**, 393-403 (1999).

8. Hamamori, Y. *et al.* Regulation of histone acetyltransferases p300 and PCAF by the bHLH protein twist and adenoviral oncoprotein E1A. *Cell* **96**, 405-13 (1999).

9. Herrmann, B.G. & Kispert, A. The T genes in embryogenesis. *Trends Genet* **10**, 280-6 (1994).

10. Crossley, P.H. & Martin, G.R. The mouse Fgf8 gene encodes a family of polypeptides and is expressed in regions that direct outgrowth and patterning in the developing embryo. *Development* **121**, 439-51 (1995).

11. Burgess, R., Cserjesi, P., Ligon, K.L. & Olson, E.N. Paraxis: a basic helix-loop-helix protein expressed in paraxial mesoderm and developing somites. *Dev Biol* **168**, 296-306 (1995).

12. Bettenhausen, B., Hrabe de Angelis, M., Simon, D., Guenet, J.L. & Gossler, A. Transient and restricted expression during mouse embryogenesis of Dll1, a murine gene closely related to Drosophila Delta. *Development* **121**, 2407-18 (1995).

13. Echelard, Y. *et al.* Sonic hedgehog, a member of a family of putative signaling molecules, is implicated in the regulation of CNS polarity. *Cell* **75**, 1417-30 (1993).

14. Sasaki, H. & Hogan, B.L. Differential expression of multiple fork head related genes during gastrulation and axial pattern formation in the mouse embryo. *Development* **118**, 47-59 (1993).

15. Ang, S.L. & Rossant, J. Anterior mesendoderm induces mouse Engrailed genes in explant cultures. *Development* **118**, 139-49 (1993).

16. Wolf, C. *et al.* The M-twist gene of Mus is expressed in subsets of mesodermal cells and is closely related to the Xenopus X-twi and the Drosophila twist genes. *Dev Biol* **143**, 363-73 (1991).

17. Ang, S.L. & Rossant, J. HNF-3 beta is essential for node and notochord formation in mouse development. *Cell* **78**, 561-74 (1994).

18. Edmondson, D.G., Lyons, G.E., Martin, J.F. & Olson, E.N. Mef2 gene expression marks the cardiac and skeletal muscle lineages during mouse embryogenesis. *Development* **120**, 1251-63 (1994).

19. Yao, T.P. *et al.* Gene dosage-dependent embryonic development and proliferation defects in mice lacking the transcriptional integrator p300. *Cell* **93**, 361-72 (1998).

20. Hogan, B., Beddington, R., Costantini, F. & Lacy, E. *Manipulating the mouse embryo - a laboratory manual*, (Cold Spring Harbor Laboratory Press, 1994).

Figure Legends

Fig. 1 Differential expression of *Gcn5* and *Pcaf* in mouse embryos. ***a-b***, total RNA was isolated from mouse embryos at the stages indicated. Northern blot hybridization was carried out using either ***a***, *Gcn5* or ***b***, *Pcaf* specific probes. *Rps*26 (ribosomal protein S26) sequences were used as an internal control. **c**, whole-mount in situ hybridization using a *Gcn5* specific probe. Arrows indicate distal allantois (8.5 dpc embryo) and the heart (9.0 dpc embryo). dpc: days post coitum.

Fig. 2 Disruption of the *Pcaf* gene. ***a***, targeting strategy for the *Pcaf* gene. A 5' exon (shown in black) in the *Pcaf* gene was deleted by homologous recombination and replaced with a SV40 polyadenylation cassette and the phosphoglycerate kinase (*PGK*)-*Neo* gene. The size and position of the targeted exon is indicated. Positions of the 5' and 3' probes for Southern blot analyses are shown. Arrows mark the orientation of the thymidine kinase (*TK*), *PGK-Neo*, or PolyA cassettes. HAT: acetyltransferase catalytic domain. Bromo: the bromodomain. P: *Pst*I; X: *Xba*I. ***b***, genotyping of *Pcaf* targeted mice by Southern blot hybridization. Mouse tail genomic DNA isolated from wild type, *Pcaf* heterozygous and homozygous mutant mice were digested with *Xba*I and hybridized with 3' probe shown in panel ***a***. The genotypes of the mice are indicated on top of the panel. The sizes of the wild type and mutant bands are indicated. ***c***, Total RNA was isolated from tissues of wild type and *Pcaf* null mice. Northern blot hybridization was performed using a *Pcaf* probe that is 3' to the targeted exon. The same blot was subsequently re-probed with a *Gcn5* specific probe and an internal control *Rps*26 probe. Arrows indicate the positions of *Pcaf*, *Gcn5*, and *Rps*26 signals.

Fig. 3 *Gcn5* null mice die during embryogenesis. **a**, targeting strategy for disruption of the mouse *Gcn5* gene. By homologous recombination, the entire *Gcn5* coding region was removed and replaced with a promoterless *LacZ* gene, which is placed under the control of the *Gcn5* promoter. ATG marks the translation start site of the *Gcn5* coding sequence. Arrows indicate the orientation of the *LacZ* and *PGK-Neo* genes. RV: *Eco*RV. ***b***, genotyping of *Gcn5* targeted mice by Southern blot hybridization. Genomic DNA was isolated from wild type and *Gcn5* heterozygous mutant mice as indicated and digested with *Eco*RV. Southern blot hybridization was carried out using the 5' probe shown in panel ***a***. The size and position of the wild type and mutant bands are indicated by arrows. ***c***, whole-mount *in situ* hybridization of a wild type and Gcn5 null embryos using a *Gcn5* riboprobe. *Gcn5* is widely expressed in a 7.5 dpc wild type embryo, but not in a *Gcn5* null littermate. ***d***, morphology of *Gcn5* null embryos at 7.5, 8.5 and 9.0 dpc. Genotypes of the *Gcn5* alleles are indicated below the embryos. Mice derived from two

independent ES cell lines showed identical phenotypes. The severity of the mutant phenotype was slightly variable. es: ectopic structure; al: allantois.

Fig. 4 Histologic and marker analyses of *Gcn5* mutant embryos. **4*a-l***, Paraffin sections were prepared from *Gcn5* mutant embryos and control littermates, and stained with haematoxylin-eosin. ***a-f***, transverse sections (proximal to distal) of a 8.5 dpc wild type embryo. ***g-l***, transverse sections (proximal to distal) of a 8.5 dpc *Gcn5* null embryo. ***m-u***, marker gene expression in *Gcn5* null embryos. Whole-mount *in situ* hybridization was performed to examine the expression of marker genes. In all panels the embryo on the left is wild type, and the one on the right is *Gcn5* null. Marker genes are indicated at the upper-left corner of each panel. Orientation of the embryos within one panel is consistent, but may vary in different panels. ***m***, *T* (*Brachyury*) is detected at the posterior end of a 8.25 dpc mutant in a pattern similar to that of the wild type littermate, but at reduced levels. ***n***, *Fgf8* is expressed at the posterior end of a 8.25 dpc mutant in a pattern similar to that of the wild type littermate. ***o***, *Tcf15* (*paraxis*) is expressed in the presomitic mesoderm and somites of a 8.5 dpc wild type embryo, but its expression is absent in a *Gcn5* mutant littermate. ***p***, *Tcf15* is expressed in the paraxial mesoderm of a 7.5 dpc *Gcn5* null embryo, although its expression is reduced compared to a wild type littermate. ***q***, *Dll1* is expressed in the presomitic mesoderm of an 8.5 dpc wild type embryo, but not in a *Gcn5* mutant littermate. ***r***, *Shh* (*Sonic hedgehog*) is expressed in the notochord and floor plate of a 8.5 dpc wild type embryo, but not in the *Gcn5* mutant littermate. ***s***, *Foxa2* (*Hnf-3b*) expression is detected in the notochord of an 8.5 dpc wild type embryo. *Foxa2* expression is detected at the distal tip and ventral lateral region of the mutant littermate, but not in the anterior midline region. ***t***, *Twist* is expressed in the head mesenchyme, somites and allantois of an 8.5 dpc wild type embryo. *Twist* is expressed in the allantois of the mutant littermate, but only very weak signal is detected in the ectopic structure and the dorsal half of the mutant littermate. ***u***, *Mef2c* is expressed in the primitive cardiac mesoderm of an 8.0 dpc wild type and its mutant littermate. al: allantois; am: amnion; cm: cardiac mesoderm; ch: chorion; es: ectopic structure; hf: head fold; hm: head mesoderm; he: heart; gd: gut diverticulum; me: mesoderm; ne: neural epithelium; ntc: notochord; ps: primitive streak; psm: presomitic mesoderm; so: somites.

Fig. 5 Apoptosis is significantly increased in *Gcn5* null embryos. Paraffin sections were prepared from 7.5 dpc wild type embryos in both (***a***, ***a1***) sagittal and (***b***) transverse orientation. ***c*** and ***d***, 7.5 dpc *Gcn5* null embryos in transverse orientation. ***e***, ***e1*** and ***e2***, 8.5 dpc wild type embryos in transverse orientation. ***f***, ***f1***, 8.5 dpc *Gcn5* mutants with both frontal and ***g***, transverse views. Extraembryonic tissues of 7.5 dpc

embryos from heterozygous matings were isolated for genotyping, and the remaining embryonic portions of the embryos were processed for TUNEL assays. Apoptotic cells are brown. Boxed areas in panels ***a***, ***e***, and ***f*** are magnified in panels ***a1***, ***e1***, ***e2***, and ***f1***. ec: ectoderm; me: mesoderm; en: endoderm.

Fig. 6 Mice null for both *Pcaf* and *Gcn5* die around 7.5 dpc. ***a***, photomicrograph of a freshly dissected 7.75 dpc litter from a $Pcaf^{-/-}$ $Gcn5^{+/-}$ intercross shows two double null embryos (arrows) with littermates. ***b*** and ***c***, histological analysis of *Pcaf Gcn5* double null embryos. Paraffin sections were prepared from double mutant embryos and control littermates, and stained with haematoxylin-eosin. ***b***, Transverse sections of 6.5 dpc *Pcaf* null *Gcn5* wild type and ***c***, double null littermates Genotyping on serial sections was performed using radioactive section *in situ*. rm: Reichert's membrane; ee: embryonic ectoderm; pc: proamniotic canal; ve: visceral endoderm; ysc: yolk sac cavity.

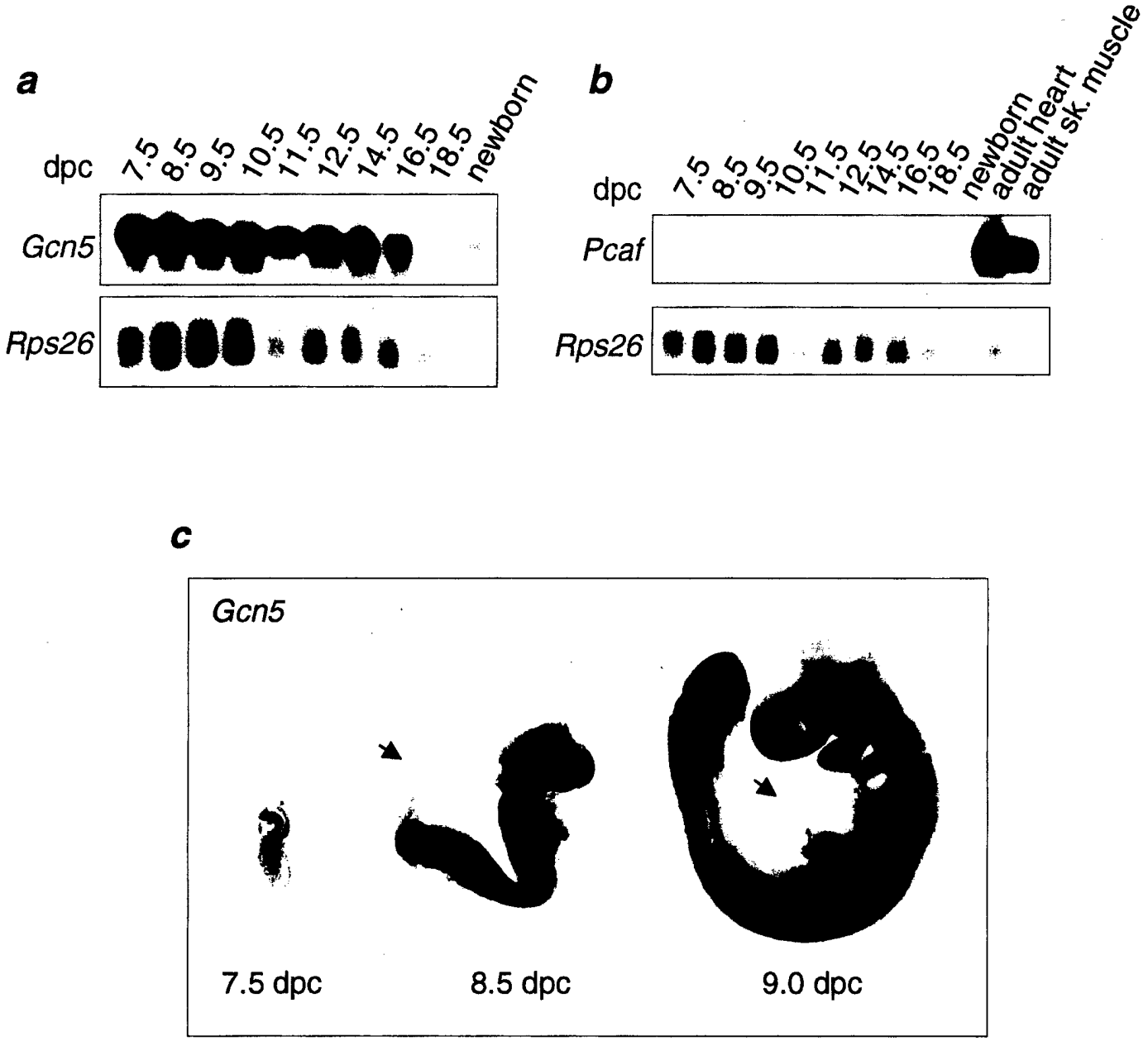
a
dpc
7.5
8.5
9.5
10.5
11.5
12.5
14.5
16.5
18.5
newborn
Gcn5
Rps26
b
dpc
7.5
8.5
9.5
10.5
11.5
12.5
14.5
16.5
18.5
newborn
adult heart
adult sk. muscle
Pcaf
Rps26
c
Gcn5
7.5 dpc
8.5 dpc
9.0 dpc

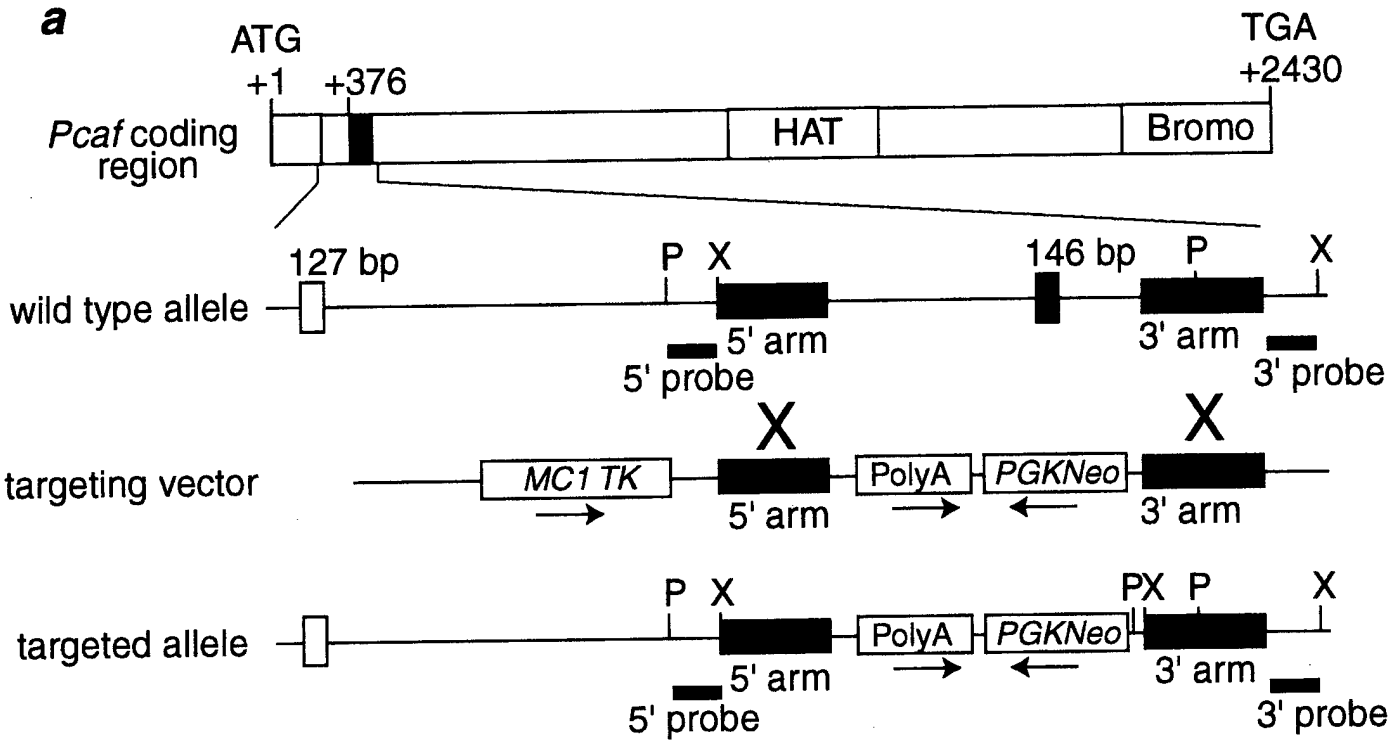
a
ATG
+1
+376
TGA
+2430
Pcaf coding region
HAT
Bromo
127 bp
P X
146 bp
P
X
wild type allele
5' arm
3' arm
5' probe
3' probe
targeting vector
MC1 TK
PolyA
PGKNeo
5' arm
3' arm
P X
PX P
X
targeted allele
PolyA
PGKNeo
5' arm
3' arm
5' probe
3' probe

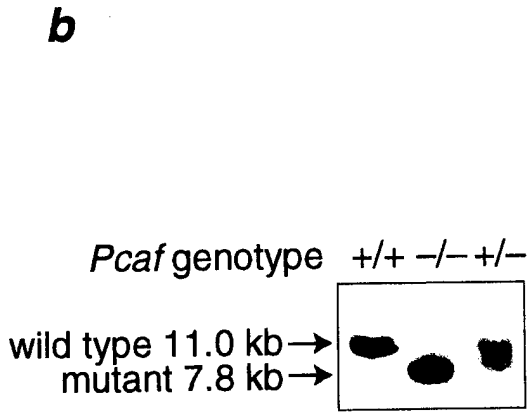
b
Pcaf genotype +/+ −/− +/−
wild type 11.0 kb
mutant 7.8 kb

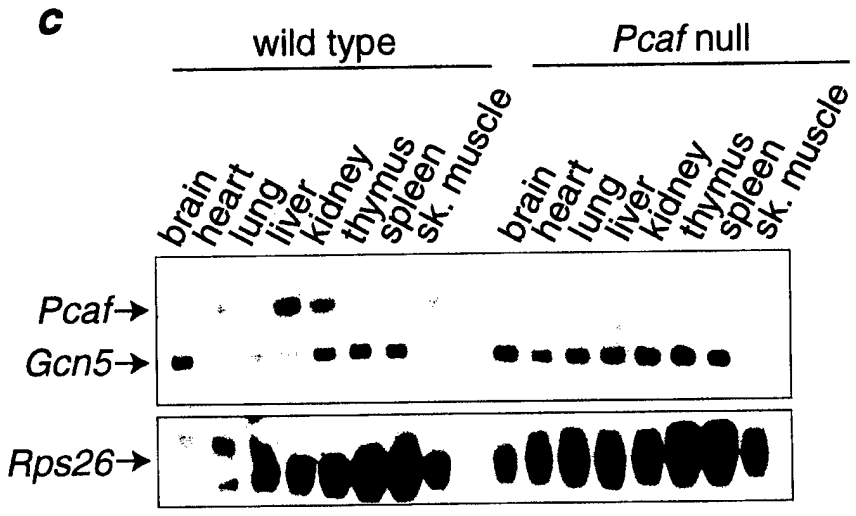
c
wild type
Pcaf null
brain
heart
lung
liver
kidney
thymus
spleen
sk. muscle
Pcaf
Gcn5
Rps26

a

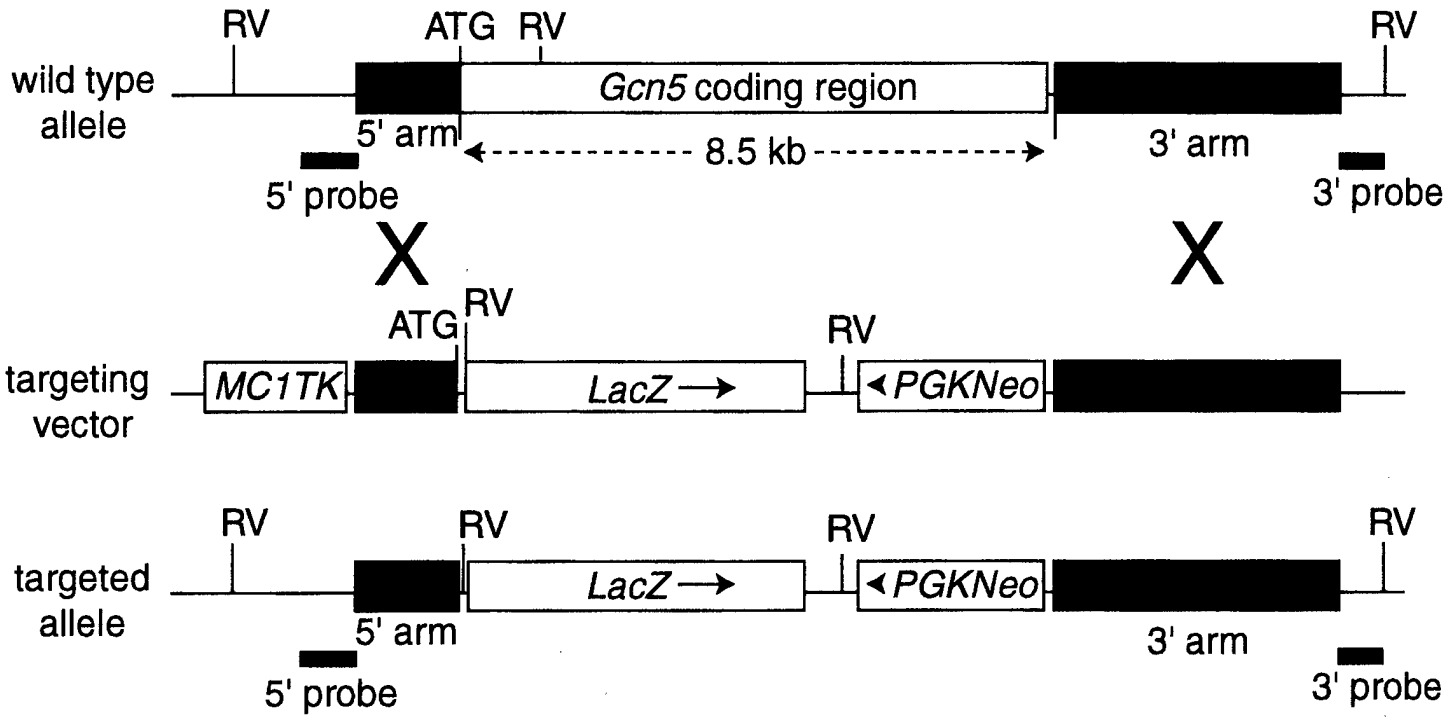
RV
ATG
RV
RV
wild type allele
Gcn5 coding region
5' arm
8.5 kb
3' arm
5' probe
3' probe
X
X
ATG
RV
RV
targeting vector
MC1TK
LacZ
PGKNeo
RV
RV
RV
RV
targeted allele
LacZ
PGKNeo
5' arm
3' arm
5' probe
3' probe

b

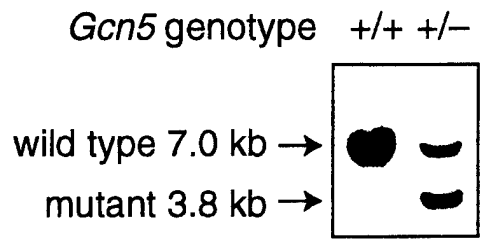
Gcn5 genotype +/+ +/–
wild type 7.0 kb
mutant 3.8 kb

c

d

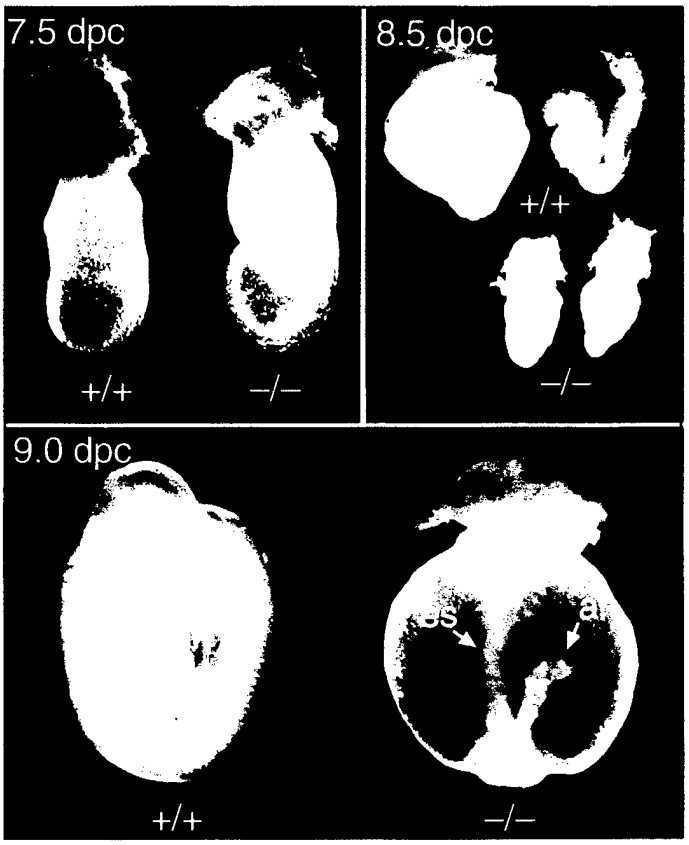
7.5 dpc
8.5 dpc
+/+
–/–
+/+
–/–
9.0 dpc
+/+
–/–

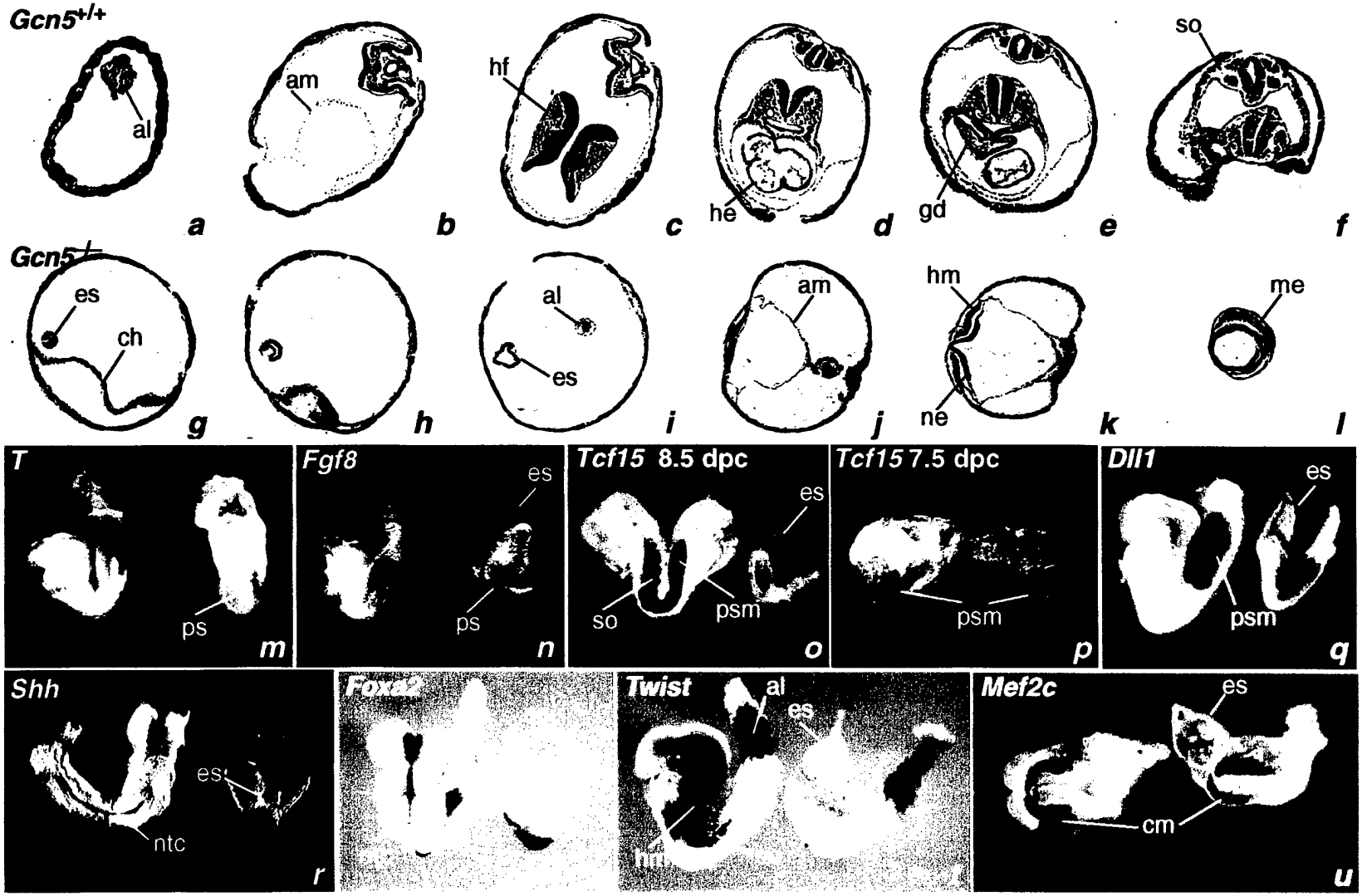
Gcn5+/+
al
a
am
b
hf
c
he
d
gd
e
so
f
Gcn5-/-
es
ch
g
h
al
es
i
am
j
hm
ne
k
me
l
T
ps
m
Fgf8
es
ps
n
Tcf15 8.5 dpc
es
so
psm
o
Tcf15 7.5 dpc
psm
p
Dll1
es
psm
q
Shh
es
ntc
r
Foxa2
Twist
al
es
Mef2c
es
cm
u

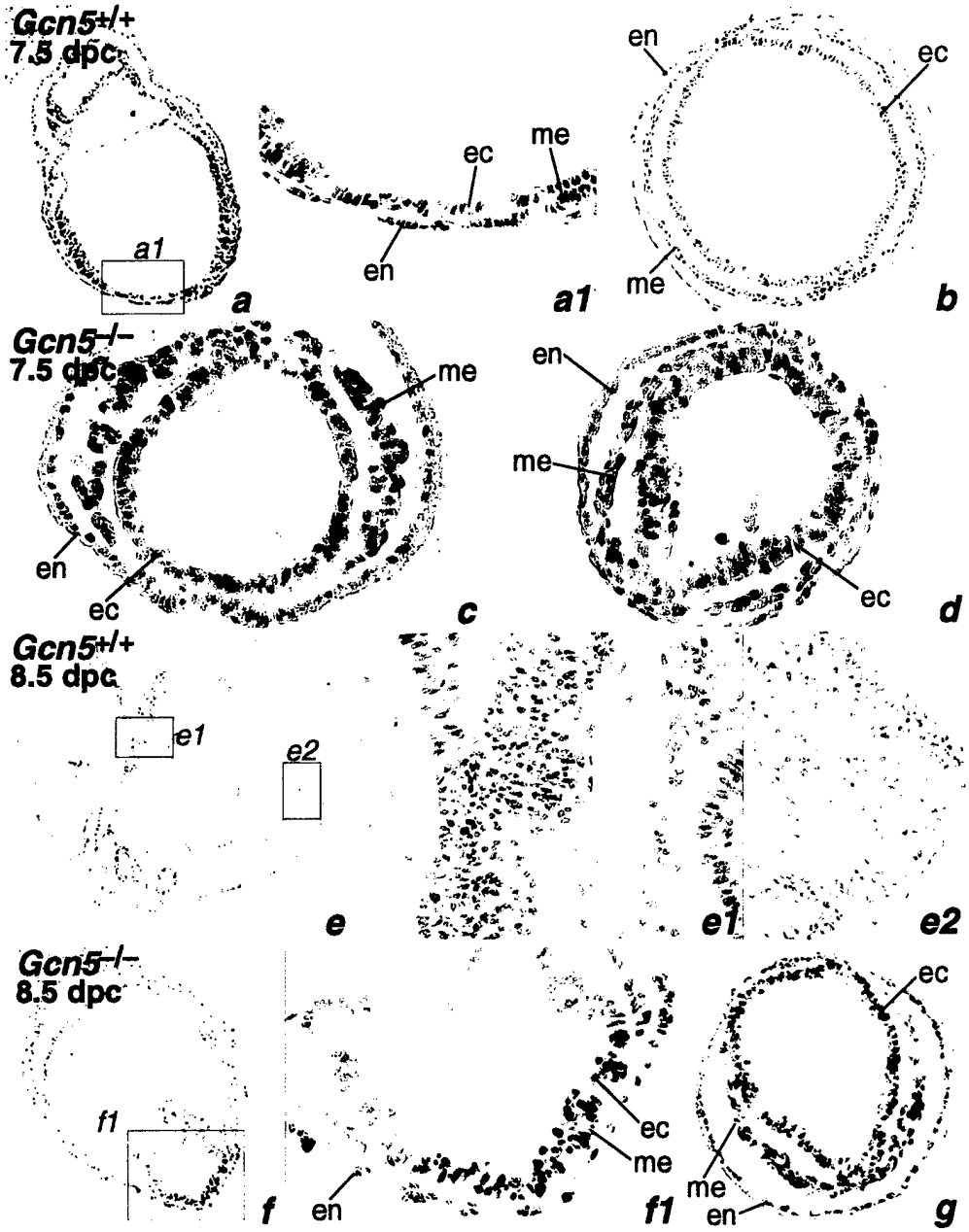
Gcn5+/+
7.5 dpc
a1
a
ec
me
en
a1
en
ec
me
b
Gcn5−/−
7.5 dpc
me
en
ec
c
en
me
ec
d
Gcn5+/+
8.5 dpc
e1
e2
e
e1
e2
Gcn5−/−
8.5 dpc
f1
f
en
ec
me
f1
ec
me
en
g

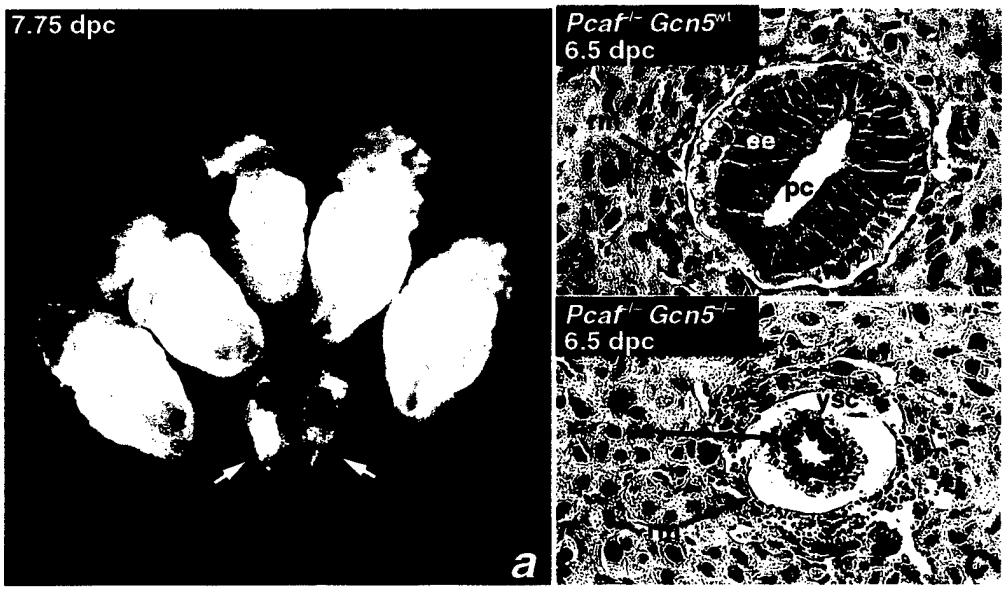
7.75 dpc
a
Pcaf-/- Gcn5wt
6.5 dpc
ee
pc
Pcaf-/- Gcn5-/-
6.5 dpc
ysc